A study of Injection Locking in Optoelectronic Oscillator

By

Prarthana Prakasha

Under the supervision of

Dr. Trevor J Hall

Thesis submitted

In partial fulfillment of the requirements for the

Master of Applied Science degree in Electrical Engineering and Computer Science

Electrical Engineering and Computer Science Department

Faculty of Engineering

University of Ottawa

Abstract

The random fluctuations of signal phase of an oscillator limit the precision of time and frequency measurements. The noise and long-term stability of the system's oscillator or clock is of major importance in applications such as optical and wireless communications, high-speed digital electronics, radar, and astronomy. The Optoelectronic Oscillator (OE Oscillator), a new class of time delay oscillator with promise as a low-phase noise source of microwave carriers, was introduced by Steve Yao and Lute Malek in 1996. The OE Oscillator combines into a closed loop an RF photonic link and an RF chain. The RF photonic link consists of a laser, electro-optic modulator, optical fibre delay line, and a photo-receiver that together provide an RF delay. An RF chain consists of one or more amplifiers and a RF resonator that together provide the sustaining amplification and the frequency selectivity necessary for single mode oscillation of the loop. The low loss of optical fibres enables the attainment of delays that correspond to optical fibre lengths of several kilometers. It is the long delay, unattainable in an all-electronic implementations that is responsible for the superior phase noise performance of an OE Oscillator.

In this thesis the fundamental principles of operation of an OE Oscillator are described and the principal sources of in-loop phase fluctuations that are responsible for phase-noise identified. This lays the ground for an exposition of the mechanism that describes the perturbation of a time delay oscillator by injection into the loop of a carrier that is detuned in frequency from the natural frequency of the oscillator. For sufficiently small detuning the oscillator can become phase locked to the injected carrier. The model presented in the thesis

generalises the traditional Yao-Maleki and Leeson model to include all the important features that describe the injection locking dynamics of an OE Oscillator. In particular the common assumptions of single mode oscillation and weak injection are removed. This is important to correctly predict the effect of injection locking on the spurious peaks in the phase noise spectrum corresponding to the side-modes of a time delay oscillator. Simulation results are presented in order to validate the dynamics of the oscillator under injection and analytic results on the lock-in range and phase noise spectrum. A 10 GHz OE Oscillator with a single 5km delay line is used as an example in the simulation illustration.

Acknowledgement

I would like to express my deep sense of thanks and gratitude for the tireless efforts and guidance of my supervisor, Dr. Trevor J Hall, from the Electrical and Computer Science Engineering Department at the University of Ottawa. During such unprecedented and troubled times his patience, guidance and above all overwhelming attitude to motivate his students to strive for excellence inspired me throughout this research. This thesis would not have been possible without his support and finally would like to thank him once again for putting up with my questions and doubts.

I thank profusely my colleagues from research group Mehedi Hasan and Minu Sunny who offered kind help and co- operation during the research period. I am extremely thankful to my senior colleagues Peng Liu and Dr. Ramanand Tewari for their advice and guidance. I also would like to express my gratitude to all the members of PT lab for their contribution to a friendly working environment.

My highest appreciations to my dear parents, Prakasha K and Mamatha K V for their constant support in every stage of my life and listening to me whenever I needed help. I also thank my sister Sanjana Prakasha for encourging and supporting me. I forever indebted to them.

Contents

List of Figures

List of Tables

List of Abbreviations

OE Oscillator	Optoelectronic Oscillator
RF	Radio frequency
PLL	Phase Locked Loop
VCO	Voltage Controlled Oscillator
SAW	Surface Acoustic Wave
IL-OEO	Injection locked Optoelectronic Oscillator
MZM	Mach-Zehnder Modulator
BPF	Bandpass filter
CW	Continuous wave
NIST	National Institute of Standard and Technology
IEEE	Institute of Electrical and Electronic Engineers
RIN	Ratio Intensity Noise
FFT	Fast Fourier Transform
SNR	Signal to Noise Ration
SL-OEO	Single Loop Optoelectronic Oscillator
DL-OEO	Dual Loop Optoelectronic Oscillator
MIL-OEO	Mutually Injection Locked Optoelectronic Oscillator
COEO	Coupled Optoelectronic Oscillator

FM	Frequency Modulation
LTI	Linear Time Invariant
PD	Photodetector
IL-PLL	Injection Locked- Phase locked Loop
LD	Laser Diode
SMF	Signal Mode optical Fiber
Q	Quality
IF	Intermediate Frequency
LO	Local Oscillator
SMSR	Side Mode Suppression Ration
SSB	Small Side Band
ICT	Information and Communications Technology
MZI	Mach-Zehnder Interferometer
FSR	Free Spectral Range

1 Introduction

Optoelectronic oscillator (OE Oscillator) has been one of the greatest invention in the recent years that is used to generate low phase noise microwave signal. An OE Oscillator is a delay line oscillator consisting of electrical and optical components that are used to generate microwave frequency signals with low phase noise, primarily the modulator. These hybrid devices contain a long, low-loss, high-qualtiy (Q) cavity optical fiber. Due to the high-Q cavity, the generation of high-frequency signal with low phase noise, which is independent of the oscillation frequency is possible. An RF circuit composed of delay lines provides means to suppress spurious resonances. The OE Oscillator setup consists of an RF-photonic link that includes a photodetector, an RF amplifier, tunable narrowband RF filter as shown in Figure 1 to provide the resonance for the oscillator. Features such as the low phase noise, high stability and high oscillating frequency are the prominent outstanding results obtained with an OE Oscillator. Such OE Oscillators are required in fields such as wireless communication, radar satellite systems, signal processing and communication systems [1]-[2].

The following research work presents the findings of injection locking of a single loop OE Oscillator. An attempt has been made to study and analyse the aspects of injection locking dynamics and the phase noise performance of single loop OE Oscillator under the influence of injection signal. This technology has an important application in the future to overcomes the limitation of traditional RF oscillator that employees frequency multiplication method to generate signals. An oscillator may be injection-locked by a carrier with frequency close to a natural frequency of the oscillator. A free-running short-

loop OE Oscillator has a relatively large magnitude phase noise spectrum, but spurious resonances can be well suppressed by its RF filter. A long-loop OE Oscillator has a relatively small magnitude phase noise spectrum, but the spurious resonances are poorly suppressed. When a strong injection signal, whose phase increment per round trip is large, is used to lock the oscillator, it can suppress the spurious resonance and can be used to reject the unwanted phase noise.

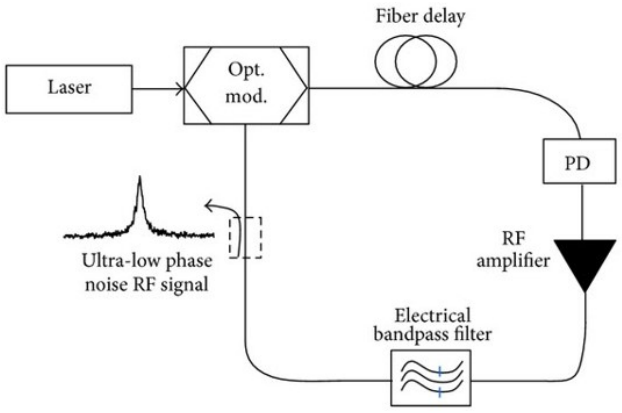

Figure 1: A block diagram of an Optoelectronic Oscillator that includes an Opt. mod: Optical modulator; optical delay line; PD: Photodetector; RF amplifier; Electrical bandpass filter. © 2013 Paul Devgan.

The injection locking of an OE Oscillator can be realised in terms of type-I Phase Locked Loop (PLL). An initial attempt to lock the OE Oscillator to a system reference using a PLL was plagued by instability. Standard PLL theory models the Voltage Controlled Oscillator (VCO) by a transfer function with a single pole at the origin, but an OE Oscillator has an infinity of poles. A more sophisticated analysis was developed to resolve instability and to predict correctly the phase noise spectrum of a locked OE Oscillator.

Even so, an RF phase shifter has insufficient range to lock an OE Oscillator against thermal drift for more than a few minutes. Practical deployment requires precision temperature controlled enclosure adding cost, bulk, and power consumption. Inspired by prior electro-optic circuits research, a breakthrough solution was conceived by Dr. T J Hall [2], that in essence replaces the polar co-ordinate system by a cartesian co-ordinate system as a solution to continuous tuning and compensation of long-term drift without loss of lock of an OE Oscillator. The innovation is to introduce components that work with Cartesian co-ordinates (x,y) on the complex plane and to avoid explicit use of polar co-ordinates (ρ,θ). Consequently the motion of the oscillator state may traverse the unit circle in either direction multiple times without dynamic range limitation to the phase or any requirement to unwrap the principal part of the phase. The concept has the merit that tuning by mode-hopping is avoided, lock maintained indefinitely over a wide temperature range and expedients to stabilisation, such as the use of tuneable lasers within a control loop or extreme temperature stabilisation measures are not required. The solution is paradigm shifting because it renders practical new strategies for substantial phase noise and spurious resonance suppression.

1.1 Background

Among a variety of means of using photonics to generate microwave signals, the concept of OE Oscillator introduced in 1996 [1] is most suited to practical deployment. The authors in [3] provides an excellent review of the literature that has arisen as a consequence of the variety of applications in which the OE Oscillators are used. Lasers and OE Oscillators are examples of time delay

oscillators. The virtue of time delay oscillators is the large delay achievable relative to the oscillation period. The low loss of optical fibre, 0.2 dB/km, permits delay line lengths of 10 km offering exceptional OE Oscillator phase noise performance. An OE Oscillator using 16 km of optical fibre can generate 10 GHz carriers with -163 dBc/Hz at 6 kHz phase noise is discussed in [9]. However, the frequency interval between adjacent oscillator modes becomes very small (20 kHz for 10 km), and filtering is needed for mode selection and side-mode suppression. Customisation to improve performance attributes, generally adversely impacts phase noise, e.g. a long loop combined with a short loop can be effective at suppressing side-modes but phase noise is compromised when compared to that of a single loop oscillator with a loop length equal to the mean of the short and long loops [19]. A model for designing a low-noise single and dual-loop OE Oscillator providing excellent agreement with experiment is presented in [4] and validated by a prototype at 10GHz frequency of 1km/100m dual loop OE Oscillator with a phase noise performance of -145 dBc/Hz at 10 kHz with spurious resonances below -100 dBc from the carrier. The OE Oscillator phase-noise at low offset frequencies is found to be driven primarily by laser frequency fluctuations mediated by dispersion. It is be possible to fully integrate a short loop OE Oscillator as a step to further stabilize the frequency fluctuation and accommodate a compact, light-weighted OE Oscillator. Although a modest off-chip optical fibre delay line is likely to remain a necessity in the immediate future to achieve the desired phase noise performance required by the most demanding applications. Over the last two decades, a considerable volume of work has been done on OE Oscillator and its different architecture to achieve the

Year and Reference	OE Oscillator Architecture	Comment	Simulation Results
Yao and Maleki 1996 [1]	Single loop OE Oscillator	Quasi-linear theory for desrcibing the properties of oscillator	Phase noise performance -140 dBc/Hz at 10 KHz offset frequency to generate 75 GHz signal
Loic Morvan 2017 [4]	Single- and Dual- loop	Physical insight to the noise coupling mechanism in the OE Oscillator loop	Highest of -160 dBc/Hz and lowest of -145 dBc/Hz noise floor achieved at 100 kHz offset frequency
David B Leeson 2015 [8]	Various OE Oscillator Architectures	Review f Oscillator Phase Noise	−145 dBc/Hz routinely obtained at VHF and low UHF frequencies
Danny Eliyahu [9]	Millimeter-wave OE Oscillator employing 1MHz high-Q optoelectronic filter	Automatic ultra-low noise floor measurement system using microwave photonic links	Phase noise of -163 dBc/Hz at 6 Hz offset for a 10 GHz carrier via 16 km long optical fiber
Zhou 2005 [16]	Injection locked Dual loop OE Oscillator	Generates Ultra-pure microwave signal with 140 dB reduction of spurious level	Phase noise level below -110 dBc/Hz at an offset frequency of 10-100 Hz
Huo 2003 [17]	Single loop with high speed NRZ signal	Carrier clock recovery at high speed	A 10-GHz clock with a timing jitter of 0.4 ps and a locking range of 800 kHz.
Yu 2005 [18]	Coupled oscillator	Ultra-low jitter clock pulse at high rates	Phase noise: -140 dBc/Hz at 10 KHz offset frequency

Table 1: Summary of research work on optoelectronic oscillators

best phase-noise performance, tunability and stability and physical size. A summary of the work done is presented below in Table 1, with reference to the ideas proposed by the authors.

1.2 Motivation

The fundamental characteristic of an oscillator is to produce high purity microwave signal with low phase noise in 1-10 GHz range [4]. In order to produce the signal at higher frequencies using traditional electronic approach different resonator technology such as crystal resonator, coaxial resonator, dielectric cavity resonator or Surface Acoustic Wave (SAW) resonator is used. However, the traditional RF oscillators requires multiple stages of multiplication to reach the GHz range, thus compromising phase noise performance at low frequencies. The RF photonic system involves RF signal generation in both optical and electrical domain, which is not possible to achieve in traditional

RF oscillators [1]. Thus, the RF photonic system is more advantageous. As a result OE Oscillator functioning as a RF photonic system proves to be an attractive option. The noise and long term stability of the system's oscillations are of major importance in application areas such as optical and wireless communications, high speed digital electronics, radar and astronomy.

Various architectures have been proposed till date to understand the principles of operation of an oscillator [4]. A stable microwave oscillation can be generated when initiated from noise if the overall linear loop gain of the oscillator is greater than unity. The envelop of the oscillation grows exponentially if the gain exceeds unity. Conversely, the envelop of the oscillation decays exponentially if the gain is less than unity. Hence the oscillator must have a gain control mechanism that stabilizes the linear gain to unity for a steady state oscillation to persist. This is the context of the Barkhausen magnitude criterion that the overall loop gain of an oscillator must be unity [3] and the Barkhausen phase criterion is that the round trip phase change must be an integral multiple of 2π, which is further discussed in the later part of the thesis.

The oscillation frequency is determined by the longitudinal modes predicted by the Barkhausen phase condition such that the frequency is within the passband. Single mode oscillation occurs, if at all it does, by winning in a competition between all the modes of energy provided by the sustaining amplifier. The oscillations in the OE Oscillator is then analyzed using quasi-linear theory. The challenge faced by every OE Oscillator is to maximize the performance by using a fibre length that will provide a high Q-factor. However, long fibre length causes oscillations of a large number of closely

packed frequency eigen modes, making it difficult for the narrow band filter to be realised at higher frequencies. One of the solutions proposed is the use of multiple loops in an OE Oscillator architecture [4]. This model introduces more than one delay line as this may lead to high spur rejection. However, the overall Q-factor is an average of the individual multiple loops, thus phase noise of the combined loops increases compared to the single loop OE Oscillator. The second solution is the injection locked OE Oscillator [7] that involves injection of an small radio-frequency electrical signal into the oscillator in order to lock the frequency tunability. The third solution would be the coupled OE Oscillator [6] that increases Q-factor and the phase noise performance of OE Oscillator by avoiding the use of an external pump laser. This configuration of OE Oscillator simultaneously generates of one short optical pulse and another microwave signal in the feedback loop [6]. Most of the aforementioned OE Oscillators are implemented with devices that make the whole setup bulky and the demand for compact size and low power consuming microwaves sources.

1.3 Objectives

With ever-increasing demand for clock frequencies being used in digital systems the requirement for compact high performance clock sources will continue. The development of such an OEO would have major impact, for example, on weather radar where very weak back-reflected signals with small doppler shifts relative to the carrier must be detected; on the generation of mm waves for 5G wireless and on the research of sources for THz radiation.

In this research, an attempt has been made to understand the various

aspects of OE Oscillator architecture, the phase locking dynamics for an injection locked OE Oscillator and noise properties in OE Oscillator loops using analytical and simulation methods. The aim is to achieve a tunable compact OE Oscillator with exceptionally low phase noise with suppressed spurious resonances and high long-term stability. Specific objectives are:

1. To understand the function of an OE Oscillator, the methods to evaluate its performance and to advance the assessment of different architectures.

2. To inform and validate theories of oscillators extended to encompass time delays, flicker noise and laser noise. To discuss about the spur suppression techniques.

3. To apply suitable proven architectures, single loop and dual loop, to ultra-low noise systems for designing an OE Oscillator under injection locked conditions and phase locked mechanism.

4. To assess the most promising architectures among the above methods by modelling, verification by simulation, and corroboration by test and measurement of discrete and integrated prototypes.

5. To understand the state-of-art of OE Oscillator through innovative architectures, phase-noise suppression and tuning methods targeting integrated solutions with phase noise <-150 dBc at 10 kHz, and comparable level spurious resonances.

1.4 Structure of thesis

The thesis is organised into 5 chapters to demonstrate the objectives mentioned above.

Chapter 1 describes the motivation and the background of the research. It summaries the research work carried out and their simulation results as a part of the literature survey. This chapter also summarizes the objectives of the thesis achievements during the period of research.

Chapter 2 introduces the fundamentals of an OE Oscillator and its architecture. This chapter contains discussion about the principles of operation for a single loop, dual loop and injection locked OE Oscillator. The OE Oscillator model contains various components having an enormous contribution on the phase noise of the oscillator. Noise contribution from various sources is discussed here. To improve the phase-noise performance of an OE Oscillator, it is important to discuss about the suppression of the spur levels and the effect it has on the quality factor.

In Chapter 3, a brief history of injection locking is produced taking inspiration from Adler and Paciorek models. This chapter introduces the concept of injection locking in an OE Oscillator with a phase locking model and also discusses how the injection locking has effects on the phase noise performance. A generalized architecture of a PLL is analyzed. Based on the proposed architecture, a theoretical approach is presented. The proposed architecture is justified by computer simulation using simulink. Furthermore, the relation between how PLL model influences the Injected Locked OE Oscillator (IL-OE Oscillator) operation is described.

Chapter 4 demonstrates the generation of the single loop OE Oscillator

with a study on the phase noise. The theoretical analysis discussed in the previous chapters is validated by computer simulation. This chapter encompasses the simulations of injection locked single OE Oscillator produced by matlab and simulink. All these simulations are backed by theoritical explaination.

Chapter 5 summarises the findings in the thesis, draws conclusions and offers recommendations for further work.

MATLAB and Simulink softwares are used to simulate all the considerations throughout the thesis.

1.5 Original Contributions and Achievements

This thesis contributes to the advancement of the noise and long-term stability of RF oscillators through analytical and experimental study of Optoelectronic Oscillators. The contributions of the author includes:

1. A breakthrough solution to continuous tuning without mode hops in an OE Oscillator and an idea to compensate the longterm drift without loss of lock are presented.

2. Currently, the prototype is compliant with the goal in terms of tuning, phase noise, locking and longterm stability and progress is being made on suppression of spurious sidemodes.

3. A critical analysis of the existing solutions to continuous tuning and experiments that have reported exceptional phase noise performance. The detailed study and analysis helped list the experimental strategies

followed by their respective author, that was studied and realised for their drawback and accountability.

4. A prerequisite to noise cancellation is the measurement of the noise. Hence, all the noise sources are studied and measured in detail using the simulations produced using Simulink software. Robust operation requires control strategies to stabilize critical components and a careful analysis of its behaviour under various conditions.

5. Further investigation can be carried out to fully integrate a short loop OE Oscillator as a step to further stability and compactness albeit a modest off-chip optical fibre delay line is likely to remain necessary to achieve the desired phase noise performance required by the most demanding applications. The challenge is the greater pathlength precision required on account of the short wavelength.

The results presented in this thesis were obtained during a period of study at the University of Ottawa from Winter 2019 to Summer 2020. The studies and discussions demonstrated in this thesis was carried out under the supervision and guidance of Dr. Trevor J Hall and PhD candidate, Mr. Mehedi Hassan at the Photonic Technology Lab (PTL).

2 Optoelectronic Oscillator

2.1 Introduction

This chapter introduces the fundamental structure and operational principle of an optoelectronic oscillator (OE Oscillator) and presents a review research on the enhancement of OE Oscillator's performance and stability. To learn about the structure of an OE Oscillator we start from the source. The OE Oscillator is fed from a laser source. The laser generates the carrier signal using an optical cavity containing an optical amplifier that acts as a gain medium to sustain oscillations. These oscillations are then modulated by an RF signal using an electro-optic modulator called Mach-Zehnder modulator (MZM) [5]. The modulated signal passes through the optical delay line that has low loss resulting in a high-quality (Q) factor RF resonator. This delayed RF signal, in the form of the envelop of an optical carrier, is then converted by a photodetector from optical to electrical domain where it is filtered using a band-pass filter and amplified using an RF amplifier. The RF coupler is used in the loop to output a fraction of the circulating RF oscillation and to feed the rest of the oscillations are fed back into the modulator to complete the loop as show in the Figure 2 [12].

The passband of the RF resonator is typically a few MHz wide which is small enough compared to a microwave or millimeter wave carrier frequency. Owing to a comparable bandwidth passband filter, the the harmonics generated by the nonlinearities, such as the ones by the Mach-Zender modulator and clipping by the RF amplifiers, are dissipated by the RF resonator. Nevertheless, the passband is large compared to the interval in frequency of the

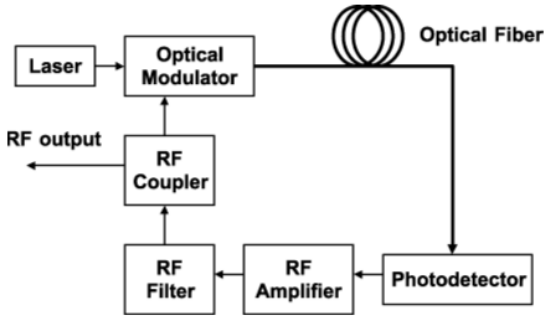

Figure 2: Block diagram of a model of Optoelectronic Oscillator (OE Oscillator). The optical fiber represents the optical delay line. The OE Oscillator setup consists of an Optical coupler where the RF output is measure [12]

infinity of possible oscillation modes provided by a delay [13]. At sufficiently small input signal levels the RF amplifier provides linear gain but at higher levels their output starts to clip, generating harmonics which are dissipated by the subsequent RF bandpass filter. The carrier generated by an oscillator has a spectrum that is broadened only by low frequency phase noise. It is therefore reasonable to assume that the RF bandpass filter is sufficiently selective to suppress the harmonics of the oscillation generated by the saturation mechanism yet has enough passband to substantially pass low frequency phase modulation without distortion [16].

An OE Oscillator, by virtue of the role played by delay in defining the possible oscillation mode is a time delay oscillator. The Barkhausen phase condition for oscillation converts phase perturbations within the loop to oscillation frequency fluctuation which is inversely proportional to the delay [17]. The low propagating loss of optical fibres enables long delays unattainable by all-electronic means, resulting in OE Oscillator as low phase noise

microwave oscillator. However, the frequency interval between the adjacent oscillation modes decreases with increasing delay to as small as 20 kHz for a 10 km long optical fibre and additional filtering for mode selection and spurious mode suppression becomes necessary [6]. By the same Barkhausen phase condition, often times the insertion of a voltage controlled RF phase shifter within the loop converts the OE Oscillator into a VCO. A phase change of 2π tunes the oscillator over one free spectral range (FSR), the frequency interval between adjacent modes.

An important property that is used to evaluate the OE Oscillator is its phase noise performance, that depends on the selection of the components. Simulating the OE Oscillator is essential to understand the design of components to achieve the required performance [4]. To achieve this we need to optimize the overall RF gain. Here are a set of parameters one needs to establish for steady-state oscillation: the continuous wave compact semiconductor laser having an optical power of P_{in} is chosen. The MZM is characterised by half wave voltage represented as V_π defining the amplitude scale [10]. The RF input from the laser to the MZM is represented as V_{in}. For a delay line length of 5 km and accordingly the fiber time delay is given by 20 μs. A microwave filter having a center frequency of 10 GHz with a 3 dB bandwidth is chosen for filtering. Finally the RF amplifier with a gain of G_a is selected such that is has lower contribution to the noise spurs and also provides enough gain for the OE Oscillator oscillations [10]. The amplitude and phase perturbation in a time delay oscillator is due to the fact that each of these parameters contribute their own phase noise. In the feedback oscillator any fluctuations of the phase of the amplifier is directly converted to frequency fluctuations

through oscillator non-linearity [26]. Ruling out technical noise which is avoidable, apart from thermal noise and small effects such as the phase noise of saturated amplifiers and photodiodes, all the significant phase fluctuations are driven by the laser Relative Intensity Noise (RIN), quantum (shot) noise, and frequency fluctuations. The RF phase noise due to laser frequency fluctuations mediated by optical fibre dispersion is a dominant mechanism at close-in carrier frequencies. Laser frequency fluctuations can also generate RF phase noise via the dispersion of discrete (multiple reflections) or continuous (double Raleigh back scattering) parasitic interferometers. This provides a window to discuss the design prototype of an OE Oscillator.

2.2 Principle of Operation

2.2.1 Optoelectronic Oscillator Prototype

The primary purpose of the OE Oscillator is to generate pristine microwave and/or millimeter wave RF carrier signals with high frequency and low phase noise. The RF amplifier provides linear gain that amplifies the recovered RF oscillation signals [20]. The amplified signal is filtered using a bandpass filter. The magnitude of the bandpass filtered output versus the magnitude of the input to the amplifier will saturate at input levels beyond the linear region and the linearized gain will approach zero suppressing any fluctuations in magnitude of the output. The amplifier filter chain operated in saturation provides a constant magnitude output signal with a phase that is a replica of the phase of the input signal filtered by the low-pass equivalent to the bandpass filter [21]. Some of the OE Oscillator configurations can be seen to

have an RF coupler. The nominally unused second input port of the same coupler may then be used to inject into the OE Oscillator an RF carrier from an external source. It is said that injection-locking can be used to improve phase noise performance but this is only true if the injected carrier has better phase noise characteristics than the free-running OE Oscillator. This quandary may be overcome by using a second OE Oscillator as the external source in a master-slave arrangement, a detailed discussed in presented in Section 2.3.2. Another possibility is bidirectional injection between two OE Oscillators. Indeed the exploration of the possibility that such architectures may be effective at phase noise and spurious resonance suppression motivated the study reported herein the next chapter of the injection locking of time delay oscillators [22].

The oscillation in an OE Oscillator can be understood on the basis of a quasi-linear theory [1]. Considering the block diagram of an OE Oscillator shown in Figure 3, let $V_o(t)$ be the output signal from the OE Oscillator and $V_{in}(t)$ is the input signal to the modulator and is given by $V_{in}(t) = V_0 \sin(\omega t + \beta)$ is applied to the modulator where V_0, ω and β are the amplitude, angular frequency and initial phase of the input signal and the relation between the input and output is expressed as [3]:

$$V_o(t) = V_{ph}\left\{1 - \eta sin\pi\left[\frac{V_{in}(t)}{V_\pi} + \frac{V_B}{V_\pi}\right]\right\} \tag{1}$$

where $V_{ph} = I_{ph}RG$ is the voltage generated at the output of the amplifier
I_{ph} is the detector photo-current at the photodetector,
η is the extinction ratio of the modulator,
V_π and V_B are the half-wave voltage and bias voltage of the modulator[3].

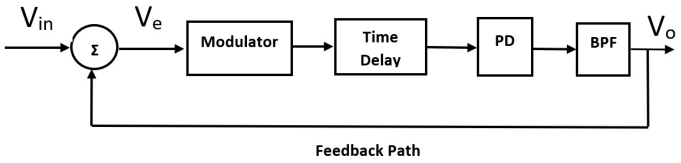

Figure 3: Block diagram of an OE Oscillator with the feedback loop

The small signal gain of the loop is calculated as [1]:

$$G_s = \frac{V_o}{V_{in}}[|V_{in}| = 0] = -\frac{\eta\pi V_{ph}}{V_\pi}\cos\left(\frac{\pi V_B}{V_\pi}\right) \tag{2}$$

This quasi-linear relationship can be established given that the bandwidth of the RF filter is sufficiently narrow enough to block all the harmonic components of the input signal. And it can be noted that the signal gain of the oscillator loop is a function of the magnitude of the input signal. Once the loop is closed, the magnitude of the oscillation increases till the gain in the oscillation mode reaches unity and then the oscillations are stabilised [23].

2.2.2 Phase noise performance

Phase noise is defined as the frequency domain representation of random fluctuation in the phase of a waveform, characterized by a spectral density that quantifies the quality of the signal's phase only. In 1978, the phase noise was defined as the ratio of the power in one sideband due to phase fluctuation by noise over the total signal power including the carrier [27]. In 1988, the Institute of Electrical and Electronics Engineers (IEEE) standard 1139 [28] defined that the phase noise is the mean squared phase deviation of the oscillator signal that exceeds about 0.1 rad^2 whenever there is a correlation

between the upper and lower sidebands of the spectral density or phase spectrum. Consider a signal at the output of the oscillator at frequency f_0, with a constant amplitude and phase fluctuation $\phi_n(t)$.

$$V(t) = V_0 cos(2\pi f_0 t + \phi_n(t)) \tag{3}$$

Considering $S_\phi(f)$ as the single side power spectral density of the phase fluctuations,

$$S_\phi(f) = \left|X_n(f)\right|^2 \tag{4}$$

where $X_n(f)$ is the fourier transform of the phase ϕ_n in equation (3). Later on by the standards and definition, the phase noise was designated as the standard measure of phase instability and is shown as

$$\mathcal{L}(f) = \frac{1}{2} S_\phi(f) \tag{5}$$

The unit of $\mathcal{L}(f)$ is dBc/Hz and it can be calculated as $10log_{10}[S_\phi(f)/2]$ or is equal to $10log_{10}[S_\phi(f) - 3dB]$ [29]. The 1999 version of the IEEE standard 1139 [30] revised that the phase noise be defined as the measure for characterizing frequency and phase instability in the frequency domain and is given as one half of the sideband spectral density of phase fluctuations. This IEEE definition also reduces the difficulty in calculating the phase noise when the angle approximation is not valid. Phase noise is used to measure the quality of the source signal frequency and is expressed in terms of figure of merit of the feedback oscillator [26], also known as spectral density or phase spectrum. The figure of merit is this case is phase noise density in dBc/Hz at a certain offset from the carrier frequency.

A feedback oscillator that consists of an RF BPF of several MHz bandwidth, admits thousands of oscillation modes. But it can favour only one

particular oscillation mode in a competition between the existing modes for the gain of an amplifier in saturation. The feedback loop is primarily tested for the phase noise measurement. The phase noise measurement has been precisely performed with phase measurement technique developed at the National Institute of Standards and Technology (NIST) [24]. The phase noise measurement equipment is commercially provided by Femtosecond system Inc that is capable of dual-channel cross-correlation measurements [25]. Meanwhile, Rubiola [29] and others have made pioneering contributions with a signal source analyzers dual channel cross-correlation are available commercially from Keysight (principal supplier), OEWaves, Rhode and Schwartz, Berkeley Nucleonics and more. Various kinds of OE Oscillator architecture has been built over the years and the best phase noise performance that has been able to achieve till date is -163 dBc/Hz at 6 kHz offset frequency for a 10 GHz microwave signal using a 16km long fiber delay line [9].

2.3 Analysis of different types of OE Oscillator model

2.3.1 Single loop OE Oscillator

A simple model for analyzing the time-averaged phase noise in OE Oscillator was developed by Steve Yao and Lute Maleki in 1996 [1]. The Yao-Maleki model assumes that the signal in the OE Oscillator, both optical and electrical is not dependent on time as their goal is only to achieve a steady state oscillations. Thus this model cannot be considered to study the noise sources and the phase noise performance, given that it does not consider the dynamic effects such as noise fluctuations, mode hopping between cavity modes, am-

plitude fluctuations and the white noise source (flicker noise). These factors has been observed to degrade the noise performance in an OE Oscillator. Given the range of parameters that needs to be considered while computing the performance of an OE Oscillator, it is important to consider an effective and accurate model to measure the OE Oscillator behaviour over the range of frequency and other parameters of interest. Hence, a single loop OE Oscillator reported here is derived from the Leeson model that invokes the same assumptions as the Yao-Maleki model but also includes a variety of phase fluctuation mechanisms [8]. The ideology behind establishing the model is to assume that a steady state single frequency oscillation is achieved and then establish a closed loop model for propagation of phase noise fluctuations. Consider the schematic setup of the single loop model shown in Figure 4.

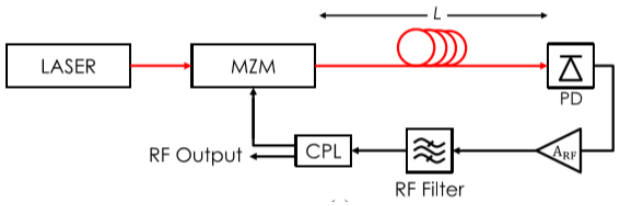

Figure 4: Single loop configuration of OE Oscillator where MZM: Mach-Zehnder Modulator; L: length of the delay line ; PD: Photodetector; A_{RF} : Amplifier gain; RF filter: Bandpass filter; CPL: Coupler.[79]

The phase noise performance of an OE Oscillator depends up on the phase coherence between the laser source and the modulator: the laser frequency fluctuations drive the RF phase noise mechanisms such as the Relative Intensity Noise (RIN). The modulator plays a minor role in determining the performance, however, it should be biased properly to maximise the modu-

lation depth. So, the phase bias drift is a major practical issue contributing thermal noise to phase performance. The fundamental photodetector noise sources are thermal noise and quantum noise. There is a 'flicker' like phenomena at high optical powers that converts RIN into RF phase due to variation in the depletion width of the photodiode. The flicker noise of a saturated amplifier via a similar mechanism (modulation of device parameters by the RF signal) is also significant. To explain the phase noise contributions consider the following block diagram in the Laplace domain from Lelivere [4]:

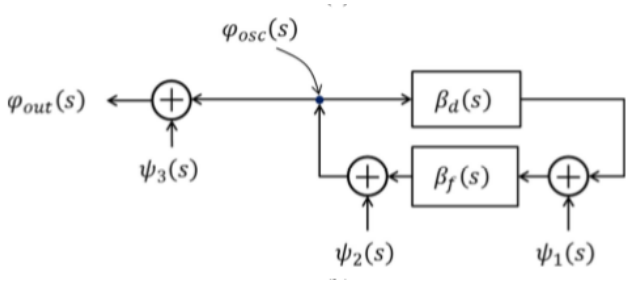

Figure 5: Laplace domain representation of an OE Oscillator with various noise sources [4]. © 2017 IEEE.

From the above Figure 5, it can be seen that ϕ_{osc} is the phase fluctuation of the input signal to the modulator, ϕ_{out} is the phase fluctuation of the output signal, β_d and β_f are the transfer function of the loop delay and RF filter respectively, ψ_1, ψ_2 and ψ_3 are the noise sources before the filter, after the filter and at the output respectively [4]. The phase fluctuation of the oscillator is given by:

$$\phi_{osc}(s) = [\phi_{osc}(s)\beta_d(s) + \psi_1(s)]\beta_f(s) + \psi_2(s) \tag{6}$$

$$\phi_{osc}(s) = \frac{\beta_f(s)}{1 - \beta_f(s)\beta_d(s)}\psi_1(s) + \frac{1}{1 - \beta_f(s)\beta_d(s)}\psi_2(s) \tag{7}$$

The power spectral density in the frequency domain can be calculated as follows:

$$S_{\phi_{osc}}(f) = \left| \frac{\beta_f(s)(2i\pi f)}{1 - \beta_f(s)(2i\pi f)\beta_d(s)(2i\pi f)} \right|^2 S_{\psi_1}(f) + \left| \frac{1}{1 - \beta_f(s)(2i\pi f)\beta_d(s)(2i\pi f)} \right|^2 S_{\psi_2}(f),$$

Since the above equation results in the oscillator phase noise power spectral density being a function of the open loop residual phase noise, the above equation can be written as:

$$S_{\phi_{osc}} = \left| \frac{1}{1 - \beta_f(s)(2i\pi f)\beta_d(s)(2i\pi f)} \psi_1(s) \right|^2 S_{\psi}(f) \tag{8}$$

where S_{ψ} the open loop phase noise from the modulator can be written as:

$$S_{\psi}(f) = \left|\beta_f(s)\right|^2 S_{\psi_1}(f) + S_{\psi_2}(f) \tag{9}$$

Thus, the phase noise at the output of the oscillator can be written as:

$$S_{\phi_{out}}(f) = S_{\phi_{osc}}(f) + S_{\psi_3}(f) \tag{10}$$

Considering the transfer functions β_d and β_f can be written as follows:

$$\beta_d(2\pi i f) = e^{-2\pi i f \tau} \tag{11}$$

where the transfer function β_d corresponds to the loop delay and hence, exhibits simple exponential behaviour driven by time delay τ. The time delay τ is the sum of the delay induced by RF component and the fiber.

$$\tau = \frac{\eta_g L}{c} + \tau_{RF} \tag{12}$$

where η_g is the fiber group index at the given wavelength [3] and the transfer function β_f can be expressed for the response to phase fluctuations [30] where

the oscillation frequency is assumed to be centered around the RF filter response.

$$\beta_f(2\pi i f) = \frac{1}{1 - 2iQ\left(\frac{f}{f_0}\right)} \tag{13}$$

where Q is the RF filter quality factor.

2.3.2 Dual loop Optoelectronic Oscillator

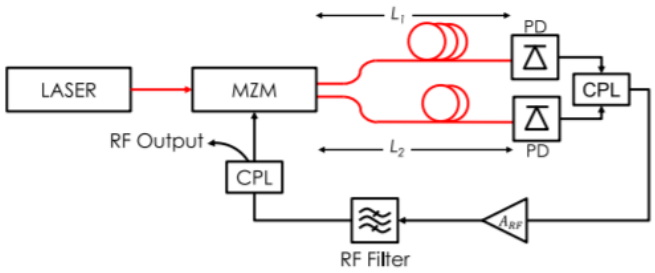

Figure 6: Block diagram of a DL-OE Oscillator to produce two signals of different delays. © 2017 IEEE

The Dual Loop OE Oscillator (DL-OE Oscillator) architecture has various implementations of which the most common types are: first is a dual output that is used to produce two signals that will experience different delays as the modulated laser light is split into two optical fibers of different length as shown in Figure 6 and second, an optical coupler is used to form two delay lines of different lengths as shown in Figure 7. In both the cases, two photodetectors convert the light signals into microwave signals that are combined using a 3 dB coupler [4]. The RF spectrum for a DL-OE Oscillator is analysed using the quasi-linear theory used for a single loop OE Oscillator. The addition of the second delay line degrades the phase noise performance

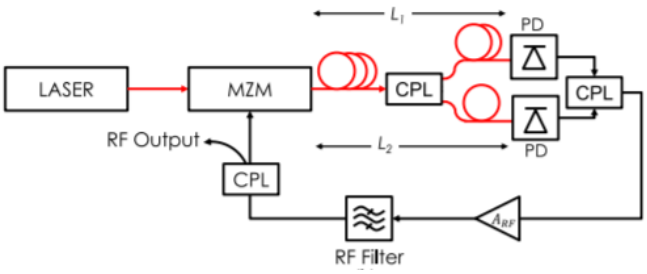

Figure 7: Block diagram of a DL-OE Oscillator with the optical coupler to split the optical delay line into a long and a short delay lines. Both these delay lines are fed to their respective photodetectors. © 2017 IEEE

slightly, however this addition decreases the height of the spur level. Using this configuration a 30 dB reduction in the noise level has been reported by the author in [47].

The overall Q factor is averaged between the long and the short loop of Figure 7, so that the phase noise increases compared to a single loop OE Oscillator. The two loops effectively form a MZM where the amplitude transmission is maximum (and in phase) when [4]:

$$2\pi f_0[(t_1 - t_2)/2] = 2\pi q \tag{14}$$

where t_1 is the delay in the long loop, t_2 is the delay in the short loop, q is a positive integer. This equation gives the Bakhausen condition for in-phase transmission. Assuming that the two photodiodes exhibit the same transfer function, and the coupler to have no phase shift, the bandpass filtering function can be written as[4]:

$$\beta_{filter}(2\pi if) = \frac{I_1 e^{-2\pi f \tau_1 i} + I_2 e^{-2\pi f \tau_2 i}}{I_1 + I_2} \tag{15}$$

where I_1 and I_2 are the photocurrent in the two photodiodes respectively.

The traditional DL-OE Oscillator, generally were made of two single mode optical fibers of different lengths and different fiber cavities, as seen above. Author in [14], introduced a new concept of using a multi-core fiber where individual single mode fibers are linked together to form a short and a long delay line separately, but under the same cavity. This method results in compact structure with increased stability and desired cavity length. This technique employs the self-polarisation stabilisation technique to avoid the unstable polarisation influence from the fibers. Prior to this an attempt was made to explore a DL-OE Oscillator based on Polarisation Multiplexing technique (PDM) involving directly combined fibers in a common polarisation beam combiner in optical domain [14]. However it is not easy to keep the polarisation state of the two fibers independent of each other under external conditions.

2.3.3 Coupled Optoelectronic Oscillator

This section introduces the concept of Coupled Optoelectronic Oscillator (COE Oscillator) operating at a frequency of 10 GHz, that consists of a coupled microwave electrical and optical loop. This type of oscillator is gaining importance because of its application in ultrahigh speed photonic signal processing for future military systems.

The coupled oscillator uses a ring laser, whose output is connected to a second coupler with a coupling ratio of 10% [11]. Most of the light from the 3-dB coupler is detected by the photodetector (PD) and amplified by the RF amplifier as shown in the Figure 8. The feedback loop here includes a variable delay line, RF bandpass filter, RF attenuator (used to adjust the

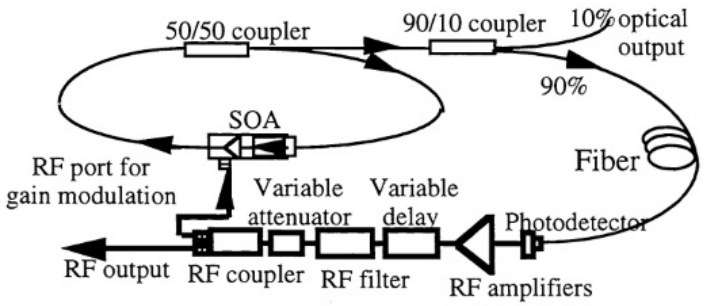

Figure 8: A block diagram representation of the coupled Optoelectronic Oscillator having ring laser [15].

loop gain) that is fed back to the modulator. The bandwidth of the filter is chosen to be narrower than the spacing beat frequency, such that the mode with the frequency closest to it gets selected [15]. In such a configuration, the length of the feedback loop is usually longer than the length of the ring laser. Hence, the centre frequency of the RF bandpass filter is chosen to be equal to the RF beat frequency of the ring laser [11]. The RF frequency closet to the natural beat frequency mode-locks the ring laser. When the laser is locked, the adjacent modes add up in phase and the frequency of the mode-locked pulse and the frequency of the RF oscillation lock to each other.

The difference between a dual loop OE Oscillator and a coupled OE Oscillator is that the second loop here is a pure optical cavity and it becomes inherent to the laser pump. And the advantage with the COE Oscillator is that it can discretely select a single mode of oscillation in the OE Oscillator even though the optoelectronic feedback loop is long. [15]. The long optoelectronic feedback loop is required for the regeneration of low phase noise RF

signals such that the mode spacing between the oscillations becomes small. This interactive regeneration becomes important for COE Oscillator mode selection. Another important characteristic of a COE Oscillator is the self-correcting mechanism [15], this property helps in stabilising the mode-locked laser output and the microwave output.

2.4 Noise contribution from various sources in OE Oscillator

During the process of designing an OE Oscillator, there are some unwanted noises that get added, for instances the noise that gets added during the conversion from optical to electrical and vise versa, during amplification and various other sources [32]. The feedback mechanism adopted in this design presents a noise floor during every loop. As a result the oscillator noise is kept in the loop at all time and the noise floor becomes a limiting factor for the measurement of phase noise performance of an OE Oscillator. The residual phase noise ψ_1, as seen in equation (6) plays a major role in determining the phase noise fluctuations. The residual phase noise can be divided between the incoherent additive noise source and power spectral density of multiplicative noise source. The additive noise can be considered as a sum of the thermal noise N_{th}, the laser relative intensity noise N_{RIN} and the shot noise N_{shot} detected by the photodiode [18], represented as follows:

$$S_{\psi_1} = \frac{N_{th} + N_{RIN} + N_{shot}}{P_{RF}} \tag{16}$$

where P_{RF} is the RF power at the photodiode output. The thermal noise, high frequency RIN induced noise and shot noise are given by the following

expressions [34]:

$$N_{th} = K_b TNF \qquad N_{RIN} = RRIN_{f_0}\frac{I^2}{4}\left|H_{f_0}\right|^2 \qquad N_{shot} = 2R_e\frac{I}{4}\left|H_{f_0}\right|^2 \quad (17)$$

where K_b is the Boltzmann constant, T the system temperature, e the electron charge, NF is the noise figure of the RF chain and RIN_{f_0} the relative intensity noise at the oscillation frequency f_0 [4]. Let us consider the various noise sources in detail:

2.4.1 Laser noise

Far more serious than the laser RIN at microwave frequencies is the low frequency fluctuations of the laser frequency. This causes a fluctuation in the delay through the group delay dispersion of the optical fibre. This directly modulates the RF oscillation frequency. Hence the phase noise of the laser is mapped directly into RF phase noise. For a single-mode laser frequency noise, there are two types of noise: intensity noise (amplitude noise) and phase noise. These types of noise arises in the laser due to the fluctuations in the optical power level. The low frequency components of the RIN and phase noise are often refereed to as 1/f noise on account of their power-law spectral density [31]. Some of the reasons for RIN induced into the oscillator circuits are cavity vibration, transferred intensity noise from a pump source or fluctuations in the laser gain medium. However, the RIN is independent of the laser power. While the RIN is not limited by the laser power, it is limited by the shot noise, which improves with increasing laser power[34]. RIN is observed to be the highest at the oscillation frequency but decreases gradually at higher frequencies until it reaches the shot noise level. This frequency set

is referred to as the RIN bandwidth. The laser RIN is measured by sampling the output current from the photodetector and transforming this data set into frequency by using a Fast Fourier Transform (FFT) or by analysing the spectrum of a photodetector signal using an electrical spectrum analyzer [32]. RIN is usually presented as the square of the optical power in dB/Hz over the RIN bandwidth at one or several optical intensities [33]. RIN of laser is thus represented as follows [33]:

$$RIN(f) = \frac{\triangle P_{opt}^2}{P_{opt}^2} \tag{18}$$

where $\triangle$ brackets represents the time averaging. In order to achieve an optimized overall RF gain, it is necessary to select a high power photodiode and a low V_π modulator [4]. However, a low V_π modulator exhibits high insertion losses. This drawback can be resolved by selecting a high power laser source.

2.4.2 Thermal noise

The thermal noise which can be observed primarily in the photodetector and voltage of thermal resistant noise, usually knowns as the white noise, can be expressed by the following equation [35]:

$$V_{Th}(f) = \sqrt{4K_bTR} \tag{19}$$

the unit is in $V/\sqrt{Hz}$, where K_b is the Boltzmann constant: $K_b = 1.38 * 10^{-23} JK^{-1}$. T is the absolute temperature (in Kelvin); R is the load resistance of the photodetector. Thermal noise is white noise over a frequency range where $hf < K_bT$. Thermal noise is observed to be constant till a

point in frequency around 10^6 Hz and then it decreases rapidly with increase in frequency due to the filtering by the BPF of the higher thermal noise of the RF chain. However, there remains a thermal noise floor due to the 50 Ohm terminations at the output coupler. The use of 50 Ohm terminations, both at the photodiode end and the RF amplifier end of the transmission line becomes the main source of thermal noise. This is done mainly for the convenience connection of discrete components and to allow oscillation frequencies over a very wide bandwidth. The thermal noise also comes from the frequency stability of the optoelectronic modulator as in [1], thermal fluctuations in the amplifier gain as described in [8], the thermal drifting of the oscillation frequency as described in [36], the temperature dependence of the refractive index of the optical fiber as in [37]. The contribution of thermal noise can be seen evidently at frequencies greater than the carrier frequency, but goes unnoticed for a spectral range close to the carrier frequency.

2.4.3 Quantum noise

The quantum noise is usually observed in the photodetector. The quantum noise contribution towards the overall phase noise of the OE Oscillator can be written as:

$$N_{shot} = 2R_e \frac{I}{4} \left| H_{f_0} \right|^2 \tag{20}$$

where R_e is the resistance of the photodiode, I is the photocurrents on the photodiode, $\left| H_{f_0} \right|^2$ is the relative microwave response of the photodiode at the oscillation frequency. Quantum noise is intrinsic to lasers and photodetectors which are the only quantum technology known that is practical at room temperature.

2.4.4 Flicker noise

The laser frequency fluctuation mainly consists of the flicker noise and the RIN. It is believed to exist because because of the non-linearity in the system, mainly the carrier. The flicker $(1/f)$ noise usually ranges from few hertz to kilohertz [38]. The flicker noise in amplifier, for instances, is due to the parametric effect on the carrier that is caused by the flicker fluctuation of the DC bias [39]. What distinguishes flicker noise is that its spectral density follows a power law. Flicker noise, a random fluctuation of the microwave carrier can be presented by the following equations [39].

$$N_{flicker} = V_0[1 + \alpha(t)]cos[2\pi f(t) + \phi(t)] \tag{21}$$

where $\alpha(t)$ is the amplitude fluctuation, $\phi(t)$ is the phase fluctuation.This equation applies to all amplitude and phase fluctuations of a carrier irrespective of the source.

The phase noise spectrum of the flicker noise has ϕ relative to time and it requires to be measured appropriately. The spectrum of a carrier with flicker phase noise will appear on a spectrum analyzers as a narrow line that appears to hop around from measurement to measurement. On a longer time scale the spectrum will average over the hopping and appear to be broader and drifting on longer time scales and so on. Although Mandlebrot managed to find a strictly stationary noise process with near 1/f characteristic (the increments of Fractional Brownian Motion are Gaussian) experimentally measured spectra contain $1/f^n$ where $n > 1$ and hence appear to be non-stationary process for which a spectral density does not exist. Nevertheless this does not stop researchers from using spectrum analysers. Hence, the

result depends on the measurement time.

2.4.5 Amplifier noise

The microwave amplifier used in the OE Oscillator closed loop circuit introduces flicker noise into the loop. The amplifier contributes to the overall noise by amplifying the non-oscillating side modes beyond 10 KHz [40]. Amplifier becomes the major limiting factor for the spectral purity of an OE Oscillator at low frequency section of the spectrum. It is characterized by a noise factor F and is expressed as the ratio of the effective noise power in the load to the noise power at the load if the amplifier was noiseless.

$$F = \frac{SNR_{in}}{SNR_{out}} \tag{22}$$

The noise factor F is defined by the IEEE standards as the measure of degradation of the Single to Noise Ratio (SNR) between the input and output of an Amplifier. And the noise figure can be represented as [41]:

$$NF = 10log(F) \tag{23}$$

2.5 Suppression of spur levels

In order to produce an OE Oscillator with high purity microwave signal and high phase noise performance, it is important to have a high Q-factor which depends on the oscillating cavity and the length of the fiber.

$$Q = 2\pi f\tau = 2\pi f\frac{nL}{c} \tag{24}$$

where f is the frequency of operation, τ is the time delay, n is the refractive index of the optical fiber, L is the length of the fiber The mode spacing of

an OE Oscillator given by $\triangle f$ can be expressed as follows:

$$\triangle f = \frac{1}{\tau} = \frac{c}{nL} \tag{25}$$

From the equation (24) and (25) it can be observed that mode spacing is inversely proportional to the length of the fiber, where as the quality factor depends upon the length of the fiber. The Q-factor of the microwave band-pass filter being used will decrease along the operating frequency and hence, making it difficult to reject the unwanted oscillation modes [6]. One of the solutions proposed to overcome this ambiguity is to introduce a dual loop OE Oscillator or injection locked OE Oscillator:

In case of dual loop Oscillator (DL-OE Oscillator), each loop has its own phase modulation and free spectral range. Hence, to achieve an oscillating mode that is suitable for both the loops and to have stable oscillations, precise measurements of the loop length is necessary. According to the author in [42] employing a polarisation beam splitter and combiner in a dual loop OE Oscillator, improved the suppression ratio by 60 dB. Since employing the dual loop OE Oscillator decreases the Q-factor and effects the phase noise performance, according to the author in [43] the spurious mode suppression can be performed while maintaining an optimum phase noise performance by controlling the gain in the oscillator. However, a more effective approach would be to let the oscillator oscillate at any given frequency and then tune the loops (a phase shifter in one of the loops) to coincidence.

A method proposed in [44], describes that the spurious mode suppression can be achieved by injecting another weak signal of compatible frequency into the OE Oscillator, which is known as injecting locking. The spur levels were about 55 dB smaller than those obtained by single or dual loop OE Os-

cillator. However, introduction of the injection signal had an impact on the phase noise performance of the oscillator. In order to overcome this limitation, author in [45] has proposed a model to study dual-injection locked OE Oscillators or mutual injection locking OE Oscillator (MIL-OE Oscillator), that operates in a master-slave configuration. By using an injection signal of injection ratio 6 dB to the oscillating signal and by increasing the slave configuration fiber loop length by a factor of 10, it is possible to decrease the spur level. To be able to have the two OE Oscillators injection locked to each other, the oscillation mode needs to be complimentary of each other and the frequencies of the oscillating mode must be close. But to be able to suppress the spurs, the frequencies of the respective oscillators side-modes must be incommensurate.

2.6 Summary

In this chapter, we studied the basic working principle of an OE Oscillator by introducing the Mach-Zender Modulator, optical delay, photodetector, RF amplifier and the RF coupler as a part of the RF chain and their noise contributions. The findings describes the properties of each of these components and a measurement methodology provides an insight to the significant contribution to the phase noise. Following which the principle of operation of an OE Oscillator was studied, that discusses the Lesson's model for a stable microwave oscillation. The procedure that is followed to build up stable oscillations is realised based on the quasi-linear theory. The relationship between each of the components with the flow of the signal is established using equations. One of the important factor that is used to measure an OE Oscil-

lator is its phase noise performance, this chapter introduced the best phase noise performances achieved till date. Single loop, dual loop and coupled OE Oscillator models are studied that describe their properties and advantages on the basis of phase noise performance. We analysed and summarised the research on various types of noise including the quantum noise and thermal noise, spurious suppression of OE Oscillator and improvement in frequency stability. Based on the properties discussed here, the following chapter will describe the injection locking mechanism in an OE Oscillator and its relation with the phase locked loop.

3 Injection and Phase locking

3.1 History of Injection locking

The evolution of an oscillator dates way back to the 20th century. After the end of second world war, promising new developments such as semiconductor devices, quantum-physics, frequency modulation, television, mobile radio communication, microwave doppler radar and space rocketry were at the budding stage of development [49]. By the 1960's, the physicists and optical engineers classified the applications of stable oscillators into two broad categories. Time precision frequency standards and metrology, expressed frequency instabilities more in the time domain terms. The other multi-signal systems such as doppler radar, radio communications and wireless communication, with their dynamic range limitations due to spectral density and availability of devices turned to frequency-domain representations and measurement. The annual symposium on frequency control which was then sponsored by the U.S. Army and by the IEEE served as a common forum for many years [49].

In electronic circuits and quantum devices the research papers focused on the RF spectrum of the oscillator and the line-width in frequency domain rather than the phase spectral density [50]. This spectral density was not in complete agreement with the complex spectra observed [51]. Frequency standards used long-term time-domain representations, radar system used short-term frequency-domain representation and a combination of both in communications as an appropriate tool of interpretation. Then the revolutionary development of the transistor, the integrated circuit, digital computing and

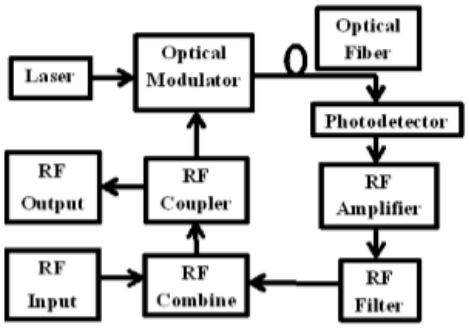

Figure 9: Block diagram representation of a injection locking model for a Single loop OE Oscillator. © 2017 IEEE

communications and space rocket gave rise to new requirements. Recent developments in the field of wireless communication and radar systems with the introduction of high frequency carriers has increased the pressure to deliver a system that can generate highly stable and low phase noise. In order to overcome the limitations faced by the electronic oscillators, optoelectronic oscillator (OE Oscillator) with injection locking was introduced as a way to stabilise the OE Oscillator [48].

3.2 Introduction

The basic block diagram of an OE Oscillator with RF input signal is shown in Figure 9. Consider a state where the oscillator is disturbed but not locked by an external signal. If the variations are rapid, tuned circuit may not be able to respond instantaneously, or in case it is a capacitor tuned circuit, it may delay the automatic readjustment of the bias voltage [52]. The grid voltage E_g, is the vector sum of the injected voltage E_L and the transformer-coupled

voltage E_0 which has the tank voltage E_F transformer coupled onto the grid.

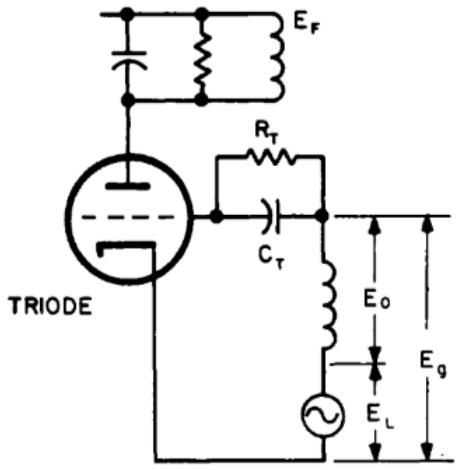

Figure 10: Alder's Oscillator circuit where R_T: Resistor; C_T: Capacitor [53]. © 1965 IEEE

In Adler's analysis, the following three important assumptions are made:

1. $\omega_0/2Q >> \triangle\omega_0$; implies that the each half of the pass band should be wider than the undisturbed beat frequency $\triangle\omega_0$, where $\triangle\omega_0$ is the difference between the impressed signal frequency and the free running frequency.

2. $T << 1/\triangle\omega_0$; implies that the time constant T should be short compared to one beat cycle, which is the inverse of beat frequency $\triangle\omega_0$.

3. $E_L/E_0 << 1$; implies that the locking signal voltage (E_L) is much smaller compared to the output voltage (E_0) and the amplitude modulation is solely determined by this ration.

The author in [54], showed that the above conditions describes the locking phenomena in reflex to the Klystron oscillator and studied the maximum modulation rate on the locking signal using the transient response of the oscillator. According to Alder's theory [52], oscillation exists provided the difference in the frequency ($\triangle\omega$) between the external injection ω_i signal and the free running oscillator signal ω_0 is always less than or equal to the locking bandwidth ω_{IL}. The phase difference between the injection signal and the locked oscillator signal is expressed as follows:

$$\frac{d\phi}{dt} = \triangle\omega - \frac{\omega_0 V_i}{2QV_e} sin[\phi(t)] \tag{26}$$

where V_i is the amplitude of the injection signal, V_e is the amplitude of the injection locked oscillator signal. In the injection locked state, the value $\frac{d\phi}{dt}$ must be zero. Then the equation becomes:

$$|\triangle\omega| \leq \triangle\omega_{IL} = \frac{\omega_0 V_i}{2QV_e} \tag{27}$$

3.3 Phase locked Loops

Phase locked loop (PLL) are used in many areas of RF design such as FM demodulators, signal re-construction, clock recovery, frequency synthesizers and many more. These synthesizers are highly stable in their frequency and allows digital lines from microprocessors circuits to control the frequency, making the PLL an excellent choice for processor-controlled system such as radio systems, signal generators and RF test equipment that requires a RF signal source. The operation of PLL is based around three main building blocks: A phase detector (PD), Voltage Controlled Oscillator (VCO) and a loop filter. This circuit also includes a reference generator outside the loop,

which is the key component for phase/frequency locking. The phase detector is the heart of the loop, it takes in the reference oscillator V_{in} and the VCO V_{out} to produce a voltage that is proportional to the phase difference between these two signals. The VCO must be monotonic i.e, with the increase in voltage there needs to be an increase in the output frequency. The condition being satisfied indicates that there is noise added in the loop. The filter with a transfer function $H(s)$ is used to shape the phase noise characteristics and loop stability.

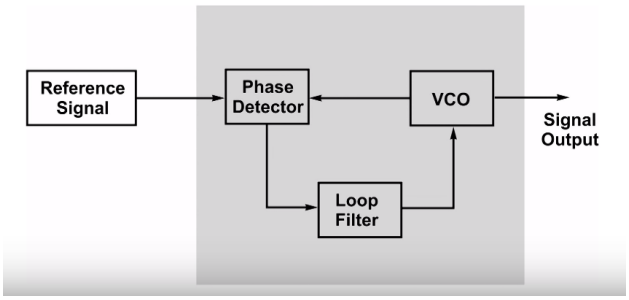

Figure 11: Block diagram representation of a Phase locked loop. © 2013 IEEE

The difference voltage produced by the phase detector is fed to the loop filter, typically a bandpass filter, to eliminate the high frequency component as shown in Figure 11 and then this signal is applied to the VCO to control its frequency. It draws the VCO frequency to the reference signal until there is steady state phase difference. When the phase difference is nearly constant, then the frequency of VCO is nearly the same as the reference signal. In this case the circuit is said to be phase locked.

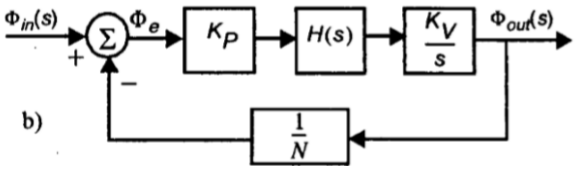

Figure 12: Phase domain representation of Type-I Phase Locked Loop. V_{in}: input voltage; PD: photodetector; H(s): Transfer function of the loop filter; VCO: Voltage Controlled Oscillator; 1/N: Frequency divider. © 2001 IEEE

3.3.1 Phase domain modelling of Type I PLL

This section presents a brief review of the basic properties of the phase-domain linear time invariant (LTI) representation of PLL. Consider the block diagram of PLL shown in Figure 12 where the input signal $\phi_{in}(s)$ generated by an external source (reference oscillator) along with the the output signal $\phi_{out}(s)$ is fed into the PD having a gain K_p, that generates an output proportional to the phase difference between the two inputs.

The control voltage (V) in an analogue type-I PLL that is directly supplied by a phase-sensitive detector that has an output given by the sine of the phase difference between the input reference and the VCO:

$$V = K_p sin(\theta_i - \theta_0) \tag{28}$$

In a phase domain model the divider is used to reduce the the VCO gain. The practical purpose of the divider is to permit a stable low frequency reference for instance, a 100 MHz quartz crystal oscillator to stabilise a much higher frequency VCO of a few GHz. Since phase is the integral of frequency and the output frequency is proportional to the control voltage, the VCO acts as an ideal integrator represented with K_v/s where K_v is the VCO gain

in Hz/Volt. An ideal divider, divides the input signal by its division ratio N and in the phase domain by a factor of $1/N$ [55]. The phase domain transfer function of Figure 12 is given by:

$$\frac{\phi_{out}(s)}{\phi_{in}(s)} = \frac{NKH(s)}{KH(s) + NS} \tag{29}$$

where K is the difference between the VCO and the PD gain, $K = K_v - K_p$. With the equations and the block diagram it can be observed that the loop dynamics can be changed by varying the transfer function H(s). In the first order loop, there exists no explicit filter [55]. The transfer function between the input and output when there is no divider used in the first order loop can be written as:

$$\frac{\phi_{out}(s)}{\phi_{in}(s)} = \frac{K_p K_v}{K_p K_v + s} = \frac{1}{1 + \frac{s}{K_p K_v}} \tag{30}$$

where $K_p K_v$ is considered as the loop bandwidth. By increasing the loop bandwidth it is possible to lower the phase error of type I PLL. The injection locking corresponds to type I PLL having proportional control for which there is a steady state phase error.

3.3.2 Injection locking dynamics of a single loop OE Oscillator

In the presence of injection, the analytic signal u representing the oscillation following the point of injection is the vector sum of the analytic signal v representing oscillation prior to the point of injection and the analytic signal

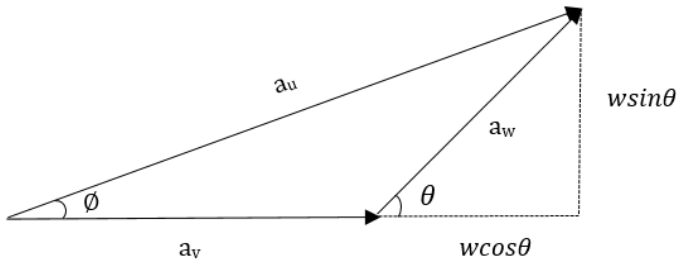

Figure 13: Cartesian coordinate depiction of the carrier signal, injection signal and the locked signal.

w representing the injection as shown in the Figure 13:

$$u = v + w, where \quad \begin{cases} u = a_u exp(i\theta_u) \\ v = a_v exp(i\theta_v) \\ w = a_w exp(i\theta_w) \end{cases} \tag{31}$$

The carrier v is a delayed replica of the oscillation following saturated gain and therefore has a magnitude that is substantially constant. The magnitude of the injected carrier w may also be taken as constant. The passband of the RF bandpass filter is sufficiently wide and the time variations of the phase fluctuations of v is sufficiently small such that the phase of the output signal of the RF filter is undistorted and equal to the phase of the input signal filtered by the low-pass filter equivalent to the bandpass-filter.

For the initial purpose of elucidating the injection locking mechanism it may be assumed that the phase of the output of the RF filter signal is substantially identical to the phase of the input of the RF filter. This assumption may be relaxed when analysing the phase-noise spectrum.

$$u = h \otimes k(u + v) \tag{32}$$

$$v < -u(t - \tau) \tag{33}$$

where τ is the delay of the optical fibre delay line, h is the impulse response of the RF bandpass filter and k is dimensionless gain constant. The gain saturation mechanism characterised by large signal gain k that decreases with increasing $|v + w|$ such that $|u|$ and hence $|v|$ are substantially held constant ($|u| = a_0$) under oscillating conditions.

Equation (31) admit a family of solutions:

$$u(t) = a_0 exp(s_0 t); \quad s_0 = \sigma_0 + i\omega_0 \tag{34}$$

subject to the condition:

$$kH(s_0)exp(-s_0\tau) = 1 \Rightarrow \begin{cases} k|H(s_0)|exp(-\sigma_0\tau) = 1 \\ \omega_0\tau - \phi = 2p\pi \qquad\qquad p \in Z \end{cases} \tag{35}$$

where ϕ absorbs the phase shift arg $(H(s_0))$ provided by the RF bandpass filter and any additional phase contributed by an intra-loop phase shift element. For $\phi = 0$ the number of cycles of the RF oscillation within the loop is an integer. The solution for a number of cycles within the delay line equal to an integer and one half correspond to $k = -1$. These negative gain solutions are a manifestation of the fact that the oscillation frequency may be tuned over a complete free spectral range by a suitable choice of ϕ in $(-\pi, \pi)$ that compensates for a fractional cycle contained within the delay line. Hence the saturated gain k is restricted in this solution to be real and positive. The

transfer function of a RF BPF placed within the loop will multiply the saturated gain modifying the magnitude and phase of the loop gain as a function of the frequency of oscillation. A suitably peaked response will favour the mode that experiences the highest initial gain leading to single mode oscillation. Assuming single mode oscillation, the effect of the magnitude of the frequency response RF BPF $|H(s_0)|$ may be absorbed into k. The oscillator freely oscillates with a natural frequency of $\omega = \omega_0$ with an envelope that with time grows exponentially if $k > 1$ and decays exponentially if $k < 1$ and remains constant if $k = 1$. The gain control mechanism will consequently maintain $k = 1$ and a steady free oscillation will occur.

$$u(t) = a_0 exp(i\omega_0 t) \tag{36}$$

In general the oscillation and the injected carrier will beat causing fluctuations of the magnitude of the vector sum but it will be assumed that its magnitude never falls below the level required to saturate the gain. This can be guaranteed for injection ratios outside unity that depends on the small signal gain and saturation power of the amplifier. Within this neighbourhood it is necessary that the phase difference between v and w is sufficient to prevent the residual signal falling below the saturation threshold during an episode of destructive interference.

In the case of a single-loop OE Oscillator it is convenient to apply the injection w at the otherwise unused input port of the RF output coupler. This corresponds to u representing the output of the coupler port driving the RF photonic link and v representing the input to the coupler port driven by the RF chain. The signal v is a delayed replica u following saturated gain and therefore has a magnitude that may be assumed under certain restrictions to

be substantially constant. The magnitude w may also be taken as constant. The injection ratio is defined by:

$$\rho = \frac{a_w}{a_u} \tag{37}$$

where a_w and a_u are the amplitudes of the injection signal and oscillating signal prior to injection locking respectively. For the initial purpose of elucidating the injection locking mechanism, it may be assumed that the phase of the output of the RF filter is substantially identical to the phase of the input of the RF filter. This assumption may be relaxed and its filtering action taken into account when analysing the phase-noise spectrum.

3.3.3 PLL interpretation of Injection Locking OE Oscillator

This section presents the analytical phase locking model based on the Adler's equation and Leeson's postulate, that is used to measure and study the phase noise performance of an injection locked OE Oscillator. The phase dynamics using Adler's equation of injection locking can be written as follows [7]:

$$\frac{d\phi}{dt} = X + \mu sin(\omega\tau) - (k + \mu sin(k\tau))sin(\omega\tau + \phi(t)) + \frac{d\beta(t)}{dt} \tag{38}$$

where X is the detuning frequency, the maximum limit of unperturbed frequency difference, $\phi(t)$ is the phase variation between the driver oscillator carrying the injection signal and the free running OE Oscillator, given by $\phi(t) = \beta(t) - \beta_0(t)$, where $\beta(t)$ is the phase variation of the injection signal and $\beta_0(t)$ is the phase variation of the carrier signal.

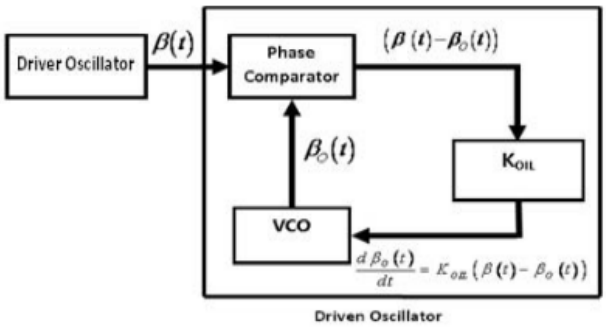

Figure 14: A model of the PLL having two inputs to the phase comparator: one from the driver oscillator and the other from the Voltage Controlled Oscillator (VCO); The K_{OIL} represents the gain [7]. © 2017 IEEE

Considering a case where the signal being injected is purely sinusoidal, then $d\beta/dt = 0$, then we obtain the equation [7]:

$$\frac{d\beta_0(t)}{dt} = (k + \mu sin(k\tau))[\beta(t) - \beta_0(t)] \tag{39}$$

where the term $(k + \mu sin(k\tau))$ represents an injection locking gain. The Figure 14 represents a block diagram of the PLL. The phase comparator included in the loop produces the phase difference between the driver oscillator containing the injection signal and the base oscillator. This phase difference is then amplified by applying the locking gain and the output of this produces the actual phase variation in an OE Oscillator driven by an injection signal [58].

Now, to study the Leeson's model, consider a stable oscillation whose output can be expressed as:

$$s(t) = a(t)exp(i\omega_0 t) \tag{40}$$

where ω_0 is the carrier frequency and $a(t)$ is the complex envelope: $a = Aexp(i\theta)$ with time varying magnitude A and phase θ. Let $a_1 = A_1 exp(i\theta_1)$ and $a_2 = A_2 exp(i\theta_2)$ be the complex envelopes of the input and output signals of a linear time invariant system then:

$$a_2 = h \otimes a_1 \tag{41}$$

where h is the impulse response of the baseband equivalent linear time invariant system . A constant magnitude signal with fluctuating phase is not bandlimited. The suppression by a bandpass filter of the spectral content of the signal results magnitude fluctuation of the envelope and distortion of the phase. The fluctuations of the magnitude may be largely suppressed by a saturating amplifier provided the magnitude of the complex envelope remains sufficiently large. The objective is then the elucidation of the action of the filter on the phase described by :

$$\theta_2 = tan^{-1}\left(\frac{h \otimes sin\theta_1}{h \otimes cos\theta_1}\right) \tag{42}$$

The fundamental postulate of the Leeson model of an oscillator is exponent conjugation:

$$h \otimes exp(i\theta) \simeq exp(ih \otimes \theta) \tag{43}$$

This is equivalent to the assertion that:

$$\theta_2 = h \otimes \theta_1 \tag{44}$$

Although this is a heuristic approximation, the Leeson postulate has proved to have remarkable utility; greatly simplifying analysis by providing a linear mapping of the phase that is accurate at least for the class of stochastic processes representative of oscillator phase noise.

To improve the long-term frequency stability of an OE Oscillator, a PLL technique to lock to an external signal with a limited loop bandwidth is being used widely.

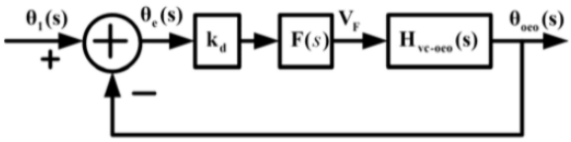

Figure 15: Phase domain representation of PLL. K_d: Phase detector gain factor; F(s): Transfer function of the loop; $H_{OEOscillator}$(s): Transfer function of the Voltage controlled oscillator. © 2016 IEEE

As shown in Figure 15, the phase domain block diagram of the Injection locked-Phase Locked Loop (IL-PLL) OE Oscillator is presented [56]. This is the dynamic representation of the PLL system in Laplace domain in an injection locking environment where the VCO has a frequency of operation ω and the free-running oscillator with frequency ω_0.

$$\omega = \omega_0 + K_v V \tag{45}$$

The phase noise of the injection locked oscillation signal given by Adler can be written as [57]:

$$\delta_{IL}(f) = \frac{cos^2\theta}{cos^2\theta + \left(\frac{f}{\triangle f}\right)^2}\delta_i(f) + \frac{\left(\frac{f}{\triangle f}\right)^2}{cos^2\theta + \left(\frac{f}{\triangle f}\right)^2}\delta_0(f) \tag{46}$$

where θ is the phase difference, f is the offset frequency from carrier, $\triangle f$ is the locking frequency range, $\delta_{IL}(f)$, $\delta_i(f)$ and $\delta_0(f)$ are the phase noises of the injection-locked oscillator, injected signal and the free running oscillator,

respectively [56]. This formula predicts a single peak around the carrier which monotonically decreases with offset frequency. This is approximately correct up to offsets of one half of the FSR.

The research proposed in this thesis predicts a phase noise spectrum that is periodic with peaks at every side mode both in the injected component and the free oscillator component. In particular, this means that the IL OE Oscillator admits noise from the external source at offset frequencies corresponding to its side-modes. This is of significance when locking two OE Oscillators together as their side modes easily coincide at some offset frequency.

$$\tau\frac{d\theta}{dt} + \left[\frac{\frac{\rho cos\theta}{1+cos\theta} + \left(\frac{\rho sin\theta}{1+\rho cos\theta}\right)^2}{1 + \left(\frac{\rho sin\theta}{1+\rho cos\theta}\right)^2}\right]\theta = 0 \tag{47}$$

when $\rho + cos\theta > 0$, the perturbations starts to decay where the sufficient condition for stability is given by:

$$\theta \in [-\pi/2, \pi/2] \tag{48}$$

3.3.4 The phase of the Injection Locked OE Oscillator

The phase $\theta_u \, \epsilon \, [-\pi, \pi]$ well-defined by the real and imaginary parts of u. The signs of the real and imaginary parts determine the quadrant and the angle within the quadrant, which is determined by the arctangent of their ratio. In order to calculate the phase of the oscillation consider the Figure 13, where :

$$u = v + w \Rightarrow a_u e^{i(\theta_u - \theta_v)} = a_v + a_w e^{i(\theta_w - \theta_v)} \tag{49}$$

where the equation (31) has been multiplied by $e^{-i\theta_v}$. The injection therefore provides an additional phase shift ϕ_i controlled by θ, the phase difference

between injected carrier and the oscillation before the point of injection. By taking the real x and imaginary y parts of the right hand side of equation (49) and then use the four quadrant :

$$\phi_i = \theta_u - \theta_v = tan^{-1}\left(\frac{\rho sin\theta}{1+\rho cos\theta}\right) \tag{50}$$

where $\theta = \theta_w - \theta_v$. The evolution of the phase of oscillation is given by:

$$\theta_v = \phi + \phi_i(t-\tau) + \theta_v(t-\tau) \tag{51}$$

Each round trip, the oscillator accumulates the increment $\phi + \phi_i(t-\tau)$ and the stair-case phase is smoothed by the convolution by the impulse response of the RF selection filter (currently omitted in the analysis). The repeated smoothing of the staircase phase results in a close approximation of a linear ramp corresponding the integrating action of a conventional oscillator, provided the gain competition successfully selects a single mode.

For small injection $\rho << 1$, equation (50) simplifies to:

$$\phi_i = \rho sin\theta \tag{52}$$

which is identical to the an analog phase sensitive detector with a phase difference $\theta = \theta_i - \theta_e$ (same as $\theta = \theta_w - \theta_v$) between the reference injection signal and signal input via an amplifier with dimensionless gain ρ driving a phase shift element induces an intra-loop phase shift ϕ_i. The oscillator converts ϕ_i via the Barkhausen condition into a change of oscillation frequency ; the time delay oscillator behaves as a phase controlled oscillator. The oscillator under injection consequently is analogous to a type-I PLL. It is advantageous to minimise the phase noise to tune the oscillator so that the quiescent phase

error is zero. Consequently, for small θ simplifies to:

$$\theta_e = \phi + \eta\theta_i(t-\tau) + (1+\eta)\theta_e(t-\tau) \tag{53}$$

where $\eta = \rho/(1+\rho)$ which identifies a more general dimensionless gain parameter $\rho < 1$ of the PLL-I model. This simple linearised model is accurate over a substantial region about $\theta = 0$.

In the special case of injection being a pure carrier of frequency ω_i, then

$$\theta(t) - \theta(t-\tau) = \omega_i\tau \tag{54}$$

and noting the Barkhausen condition for the equilibrium free-oscillation at the nominal reference frequency:

$$\theta(t) - \theta(t-\tau) = \omega_0\tau - \phi \tag{55}$$

Substituting equation (50) in the above equation and integrating the left hand side:

$$\tau\frac{d\theta}{dt} = (\omega_i - \omega_0)\tau - tan^{-1}\left(\frac{\rho sin\theta}{1+\rho cos\theta}\right) \tag{56}$$

which is equivalent to the Paciorek equation adapted to a time-delay oscillator. Most of the time applying Adler's theory to an OE Oscillator fails to account for the side modes in the lock-in range and the phase noise spectrum. Since the OE Oscillator is treated as a single mode oscillator, the multi-mode nature of a time delay oscillator is only accounted for in the difference equation as shown below:

$$\tau\frac{d\theta}{dt} = (\omega_i - \omega_0)\tau - \frac{\rho sin\theta}{1+\rho cos\theta} \tag{57}$$

When the OE Oscillator is presented with weak injection signal, the injection ratio $\rho \to 0$, by equating injection ratio ρ to the dimensionless gain k, the

above equation reduces to:

$$\tau\frac{d\theta}{dt} = (\omega_i - \omega_0)\tau - ksin\theta \tag{58}$$

3.4 Summary

This chapter summarises the injection locking procedure in a single loop OE Oscillator. The main idea of this chapter is to understand the fundamentals of PLL and IL and establish a relationship between the two. It considered the interpretation of a single loop OE Oscillator subject to injection locking in terms of the phase locked loops. We looked into the history of injection locking, particularly discussing Adler theory that suggests the need for frequency difference to exists between the free running oscillator and the reference signal to initiate the process of injection locking. Further we investigated the conditions for bandwidth, time constants and derived the equations of phase as function of time. This chapter used the fundamentals of PLL to understand the design of a compact PLL interpreted IL-OE Oscillator with standard off-the-shelf transfer function and gain. The injection locked OE Oscillator obeys the Barkhausen's condition to behave as phase controlled oscillator. Using these interpretation and design model, we can simulate an OE Oscillator with injection signal; thus helping us create a delay line oscillator that satisfies stable oscillation conditions.

4 Simulation studies

4.1 Introduction

A major advantage of the combination of the optical and electrical components to build an Optoelectronic Oscillator (OE Oscillator) is the versatility of the architectures that can be reconfigured to achieve the best performance, optimal size, cost and power consumption. The essence of such oscillators lies in the long length of the fiber that results in long fiber delay and hence, high spectral purity [59]. The aim is to simulate results for a compact and low noise OE Oscillator at 10 GHz.

Time and frequency domain simulations have been conducted to verify theoretical predictions. Simulink and Matlab are used to implement time- and frequency- domain models respectively. There are two varieties of time-domain models. The first variety represents the oscillation by its analytic signal. Without loss of generality, it is the complex envelop of an implicit pristine carrier corresponding to some natural frequency of oscillation that is simulated. This is equivalent to translating in frequency the analytic signal to baseband or zero carrier frequency [62]. The complex envelop representation is motivated by the sample rate required in a digital simulation to avoid aliasing. The complex envelop requires a sample rate at least equal to its extent in the frequency domain which is of the order of 1 MHz at most whereas to adequately represent the same analytical signal with an explicit carrier requires sampling of the order of 10 GHz.

The device of a complex envelope representation used with advantage in optical circuit simulators to avoid having to sample an optical carrier

which has a frequency of the order of 200 THz [63]. It is tempting to use an optical circuit simulator to simulate an OE Oscillator to take advantage of the sophisticated component models for lasers, modulators, optical fibres, photodetectors and a more limited range of electronic components. However, the number of samples required to adequately represent the RF modulation in transit through a fibre loop of length of the order of 10 km is prodigious ($\sim$ 100,000) and simulations of oscillators with coil lengths of up to $\sim$ 100 m is possible before exhausting available computing resources. This problem is avoided by treating the RF-photonic link as an RF delay line, indeed the purpose of the photonics is to transport the RF carrier over a long path taking advantage of the low loss of the optical fibre [64]. Ideally, the photonics could otherwise be ignored. However, the photonics does contribute to the RF phase noise spectrum by a variety of mechanisms.

4.2 Simulations with Matlab

Simulating the OE Oscillator is fundamental to understand the dynamic behaviour, mode hopping, amplitude changes and phase noise fluctuations. With regards to a brief history on simulating the OE Oscillator model, a prominent one is based on the the phase noise analysis by Lelievre [4], a number of simulations including the time-averaged phase noise dependence on frequency offset of the carrier signal, the length of the optical cable and the oscillation power were produced [60]. However, the disadvantage of this model is that it does not consider the time-dependent dynamic effects of the model, which can eventually degrade the operations and performance of an OE Oscillator. A number of attempts have been made to take into account

the time dependent dynamical effects. First among them was produced by Chembo based on delay differential equations [10]. Another model was proposed by Levy implementing dynamic effects [46] that includes three different frequency scales: first is of a few gigahertz of the output RF signal frequency, second is of the order of hundreds of kilohertz in the cavity mode spacing and third is of several to thousands of hertz in the frequency offset of the phase noise. Frequency scale of the order of 100 THz corresponding to the carrier frequency of the light in the OE Oscillator's optical fiber may also be used [66].

4.2.1 Single Loop OE Oscillator: Time domain model

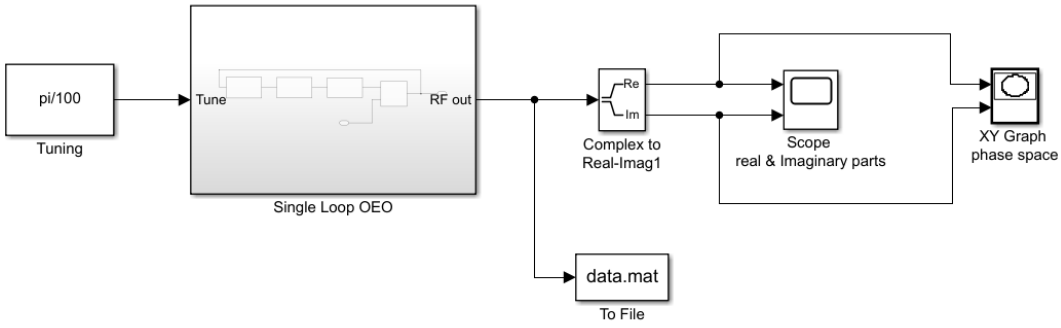

Figure 16: Block diagram of a Simulink model of a single loop OE Oscillator and test harness.

In this research, originally it was hoped that the phase noise spectrum could be assessed by appropriate spectral analysis of time domain models. However, the noise floor due to the finite precision of simulink solvers proved too great to model phase noise at the levels $\sim$ -150 dBc/Hz of interest.

Consequently, phase noise performance is assessed using frequency domain models simulated by Matlab. This observation reaffirms the rationale for using Simulink rather than an optical circuit simulator for the time domain simulations. Nevertheless the envelop models are built from blocks close rather than abstract descriptions of the component parts that form an OE Oscillator.

Figure 16 shows the top level block diagram depiction of a single loop OE Oscillator (SL-OE Oscillator). The frequency of the OE Oscillator is tuned relative to the nominal reference frequency via the constant input to the 'single loop OE Oscillator' block. The oscillation frequency is tuned over one free spectral range (FSR) for an input provided by the 'tuning' block. The RF output is a complex amplitude time series. The in-phase (real part) and quadrature phase (imaginary part) components are displayed over time as waveforms by the 'scope' block having two inputs and as a trajectory in phase space by the 'X-Y Graph' block. The complex time series is also logged by the 'To file' block into a data file for further analysis.

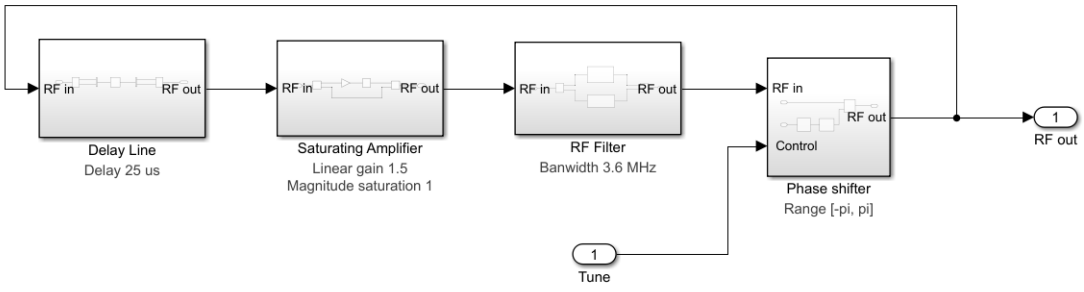

Figure 17: Details of the Single loop OE Oscillator block shown in Figure 16

A detailed look on contents of the 'Single loop OE Oscillator' block is shown in Figure 17. This block consists of a 'delay line', 'saturating amplifier', 'RF filter' and 'phase shifter' in a loop that form the oscillator and provides the output via the RF out port. The phase shift provided by the 'phase shifter' block is controlled via the 'tune' port. Each of these blocks is further explained below.

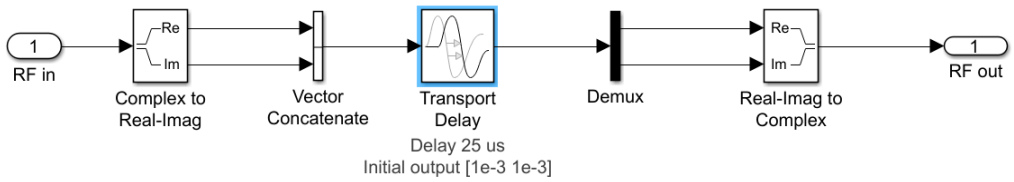

Figure 18: Details of the delay line block

Figure 18 shows the inside content of the 'delay line' block. This fundamentally makes use of the supplied 'transport delay' Block. The latter does not support complex data types but it does support real vectors. Consequently it is necessary to precede the 'transport delay' block by the 'complex to real-imag' block and 'vector concatenate' block to assemble the real and imaginary parts of the complex RF into two components of a real vector input to the transport delay. The 'demux' and 'real imag to complex' blocks reassemble the real vector output of the 'transport delay' into the complex RF out. A small initial output is used to emulate a power on transient to initiate oscillation. The oscillator will start-up from a small amount of noise injected into the loop in which case this initial condition may set to zero but then the simulation time required to reach a fully developed oscillation can be prolonged.

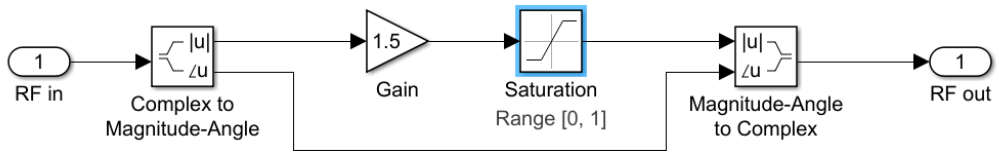

Figure 19: Details of the saturating amplifier

Figure 19 shows the detail component composition of the 'saturating amplifier' block. The 'complex to magnitude-angle' and 'magnitude-angle to complex' blocks create two paths: one for the phase and the other for the magnitude. The phase path is straight through ensuring that the phase of the output of the amplifier is the same as the input. The magnitude is however amplified by the 'gain' block which provides the small signal gain and then hard limited by the 'saturation' block which emulates the fast hard clipping of a saturated RF amplifier. The model does not generate any harmonics consistent with the assumption that these are all dissipated by the bandpass response of the RF amplifier and bandpass filter chain.

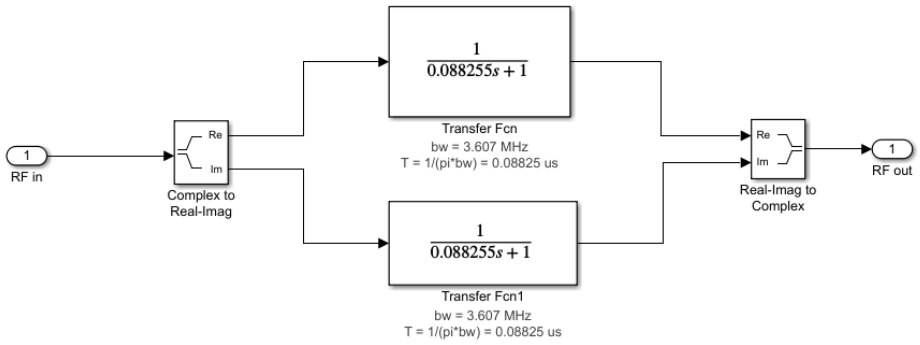

Figure 20: Details of the RF filter block.

Figure 20 shows the detail component composition of the 'RF filter' block. The complex envelope representation maps the passband centre frequency of an RF bandpass and hence to an equivalent low-pass filter. The low-pass filter is fundamentally based on the supplied 'transfer fcn' block, which only supports real data types. It is therefore necessary to use 'transfer fcn1' block that is identical to 'transfer fcn' blocks that separately act on the real and imaginary parts of the complex envelope. This is accomplished with the aid of the 'complex to real-imag' and 'real-imag to complex' blocks.

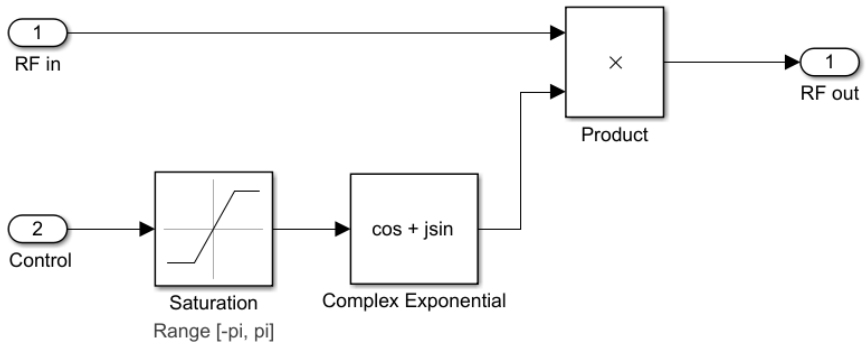

Figure 21: Detail of the Phase Shifter block

Figure 21 shows the detail component composition of the 'phase shifter' block. The input from the 'control' block is limited to $[-\pi, \pi]$ by the 'saturation' block to emulate the limited range of a phase shifter. The phase is then converted by the 'complex exponential' block to its equivalent transmission which multiplies the 'RF in' complex envelope to provide the 'RF out' complex envelope.

4.2.2 Results

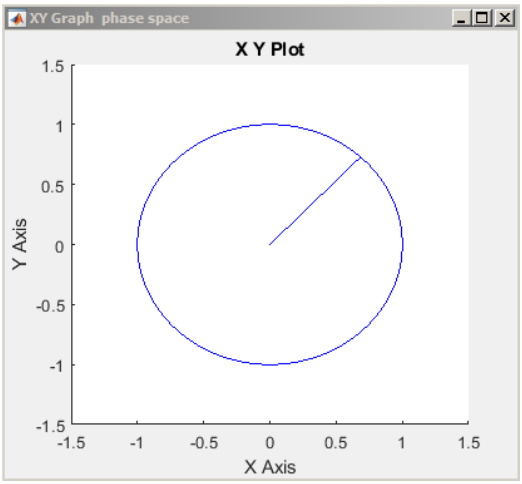

Figure 22: The X-Y plot result provided by the single loop OE Oscillator simulation

Figure 22 shows the XY plot as shown as the output in Figure 16. The almost radial line describes the exponential growth from the initial power on transient. The circle describes the limit cycle in phase space of the ensuing oscillation. During the simulation the direction of motion around the circle is clear: anticlockwise for a positive tuning phase corresponding to a positive frequency and clockwise for a negative tuning phase corresponding to a positive frequency of oscillation relative to the reference.

Figure 23 shows the in-phase (real) and quadrature phase (imaginary) components of the complex envelope provided by the single loop OE Oscillator simulation over a time duration from start-up of 100 ms. The small steps in the waveform is not a plotting artefact but a real feature of a time delay oscillator for which the phase progressed initially as a staircase which

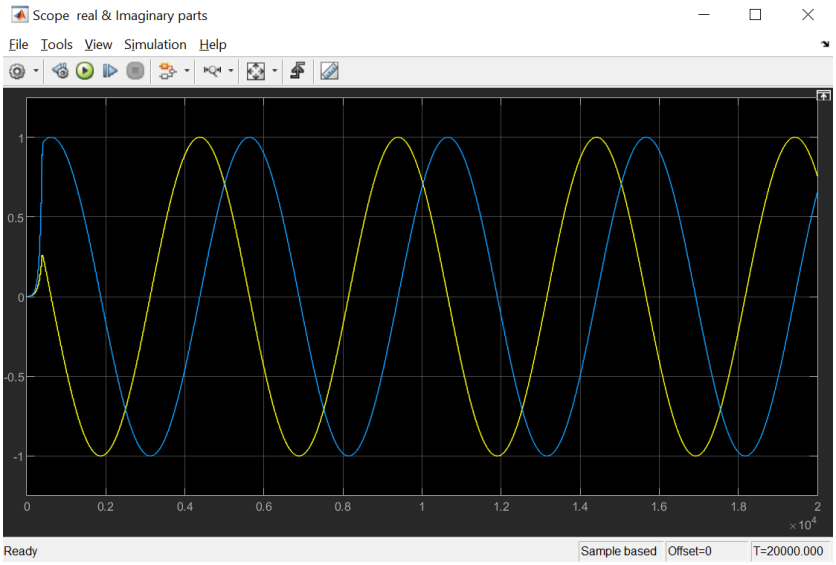

Figure 23: The real and imaginary parts of the complex envelope of a Single loop OE Oscillator

is gradually smoothed by the action of the RF filter.

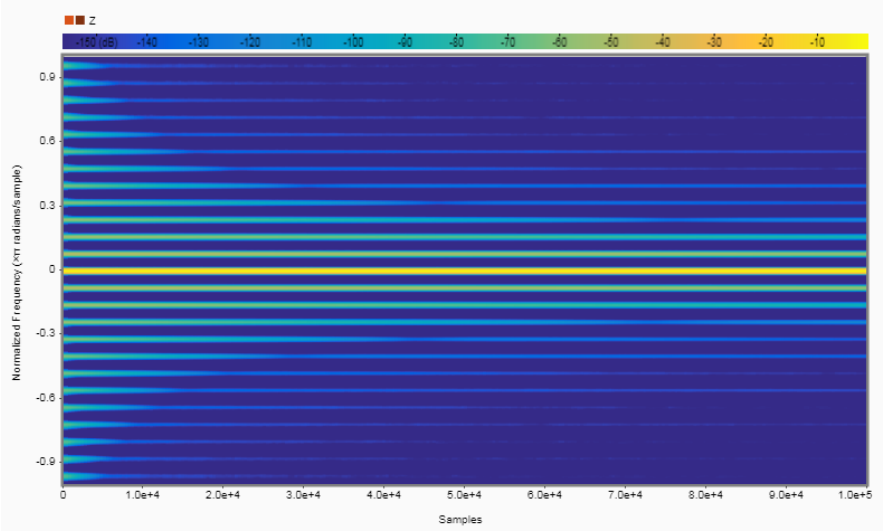

Figure 24: A spectragram of the data of a Single loop complex envelope

Finally, Figure 24 shows a spectragram (short time fourier transform) of the data shown in Figure 23 provided by the Matlab Signal Analyzer application. The vertical axis is the short time frequency and the horizontal axis is the simulation time. The numbers given on calibration bar for the colours are in decibels. The bright orange horizontal line close to zero frequency corresponds to the fundamental oscillation mode. The adjacent blue lines correspond to the adjacent side modes that are excited at a relative level of -100 dB by the initial transient and are reflected in the small steps in the waveforms shown in Figure 23. These side modes can be seen to decay with increasing simulation time as a result of the smoothing provided by the RF filter.

4.2.3 Injection locking OE Oscillator simulation

The injection locked OE Oscillators are realised by self-injection of the output signal to a long delay line. The resulting reduced phase noise was recorded at -120.1 dBc/Hz (4-dB phase-noise reduction) at 1-MHz offset for 9.6-GHz band by Leeson in 2015 [8], -50 dBc/Hz (20-dB phase-noise reduction) at 10-kHz offset for 8-GHz band by D. Eliyahu in 2008 [9] and -95 dBc/Hz at 100-kHz offset for 60-GHz band by ceramic high- resonator in the loop was achieved by Chembo in 2008 [10]. It is possible to achieve better phase noise in the RF domain using a longer delay line, however the longer delay line is limited by large loss and increased oscillator frequency noise. The use of high Q external resonator can improve the oscillator filtering function, but results in increased noise. However, it is possible that we use long delay lines of optimal length to produce high-Q external resonator in injection locked

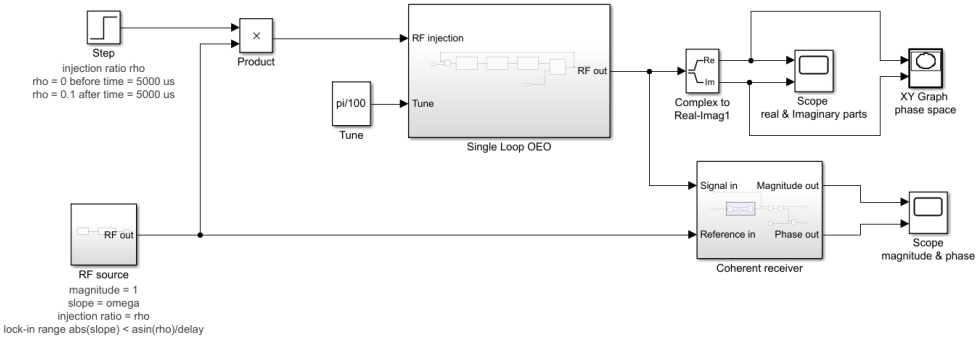

Figure 25: Detailed single loop OE Oscillator equipped with an RF injection port and the injection locking harness.

oscillators such that it reduces the transmission loss of optical fiber as shown in [60]. One another prominent method to significantly reduce the output phase noise is by injection locking with the optical loop acting as feedback loop [61]. This method reported by Lee in [61], successfully demonstrates a single-mode oscillation at 30-GHz bands with a side mode suppression ratio (SMSR) larger than 50 dB. The output phase-noise reduction of about 18 dB at 10-kHz frequency offset was achieved.

To study the injection locking mechanism consider the envelope model simulations shown in Figure 25. With respect to the basic SL-OE Oscillator configuration seen in Figure 16, this figure explains the injection locking model that consists of an RF injection source. The 'RF source' provides a complex envelope corresponding to the RF carrier to be injected. The 'step' and the 'product' block together act as an amplitude modulator that sets the injection ratio ρ to zero before a specified time and to a specified value afterwards. In this example the step occurs at 5000 μs and is of height $\rho =$

0.1. The coherent receiver measures magnitude and phase of the single loop OE Oscillator 'RF out' relative to the RF source. This enables detection of lock, loss of saturation and evaluation of the asymptotic phase.

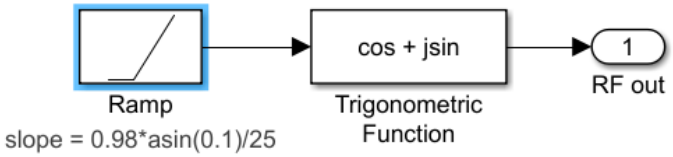

Figure 26: Detail of the RF source block

The 'ramp' and 'trigonometric function' blocks provide an RF out envelope u of the form $u = exp(i\omega t)$, as shown in Figure 26 where u is RF output. An addition of the 'add' block to the 'single loop OE Oscillator' block can be seen in Figure 27. The 'add' block has input ports: one for the RF injection and the other port acts as a feedback port. The 'tune' port inputs to the 'phase shifter' block that is used for a constant value of $\pi/100$.

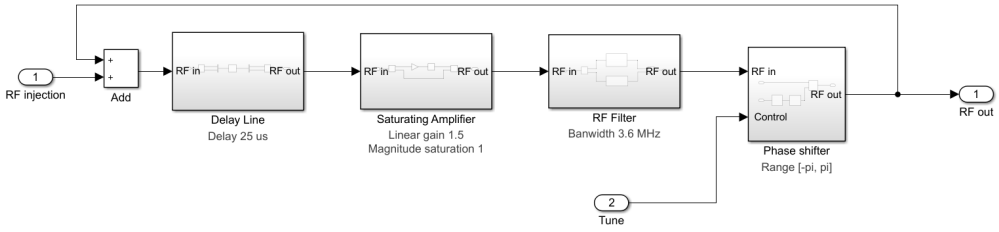

Figure 27: The Single Loop OE Oscillator block.

Figure 28 shows the detailed architecture of the 'coherent receiver' block. The heart of the circuit is the four quadrant 'product' block which emulates

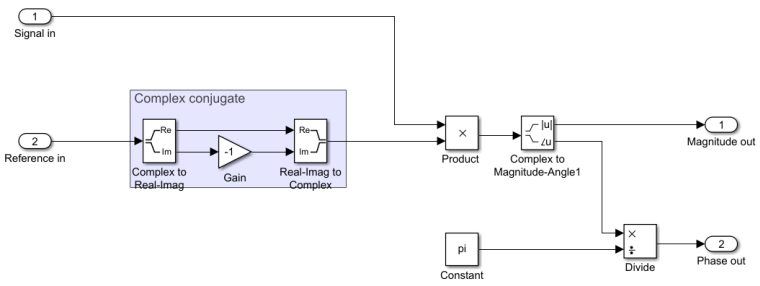

Figure 28: Detail of the Coherent receiver block.

a mixer. The 'complex conjugate' subsystem block acts on the 'reference in' complex envelope ensuring that the Signal in complex envelope is down converted by the mixer to a baseband and its magnitude and phase passed to the output ports. For convenience the 'constant' and 'divide' blocks normalise the phase to units of π radians.

4.2.4 Results

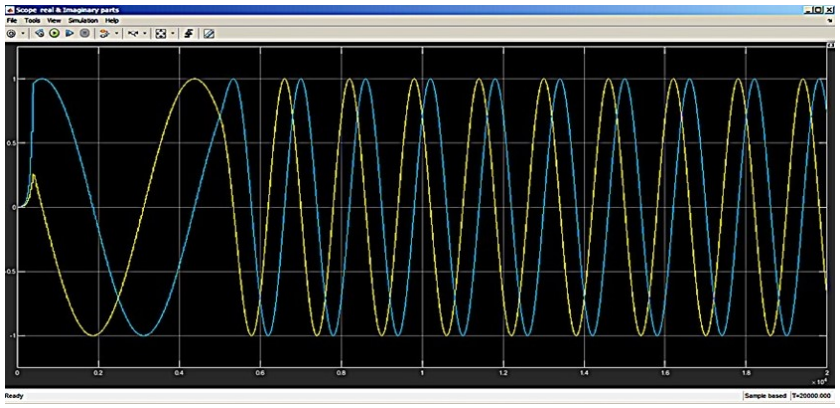

Figure 29: Real (yellow) and imaginary (blue) parts of the OE Oscillator RF out complex envelope under injection.

After analyzing the injection locking model, the following presents the simulation results of the injection locking model under different injection ratio conditions. From Figure 29 it can be seen that for the first 5000 μs the oscillator is free, thereafter the RF source is injected with injection ratio ρ=0.1. For clarity of visualisation the OE Oscillator has been detuned by $\omega\tau = \pi/100$ where τ=25 μs is the delay so that the free oscillation corresponds to a longer period oscillation. The RF source is detuned to 98% of the high frequency limit of the locking range $\omega\tau = sin^{-1}(\rho)$. It is observed that locking is successful with this configuration parameters.

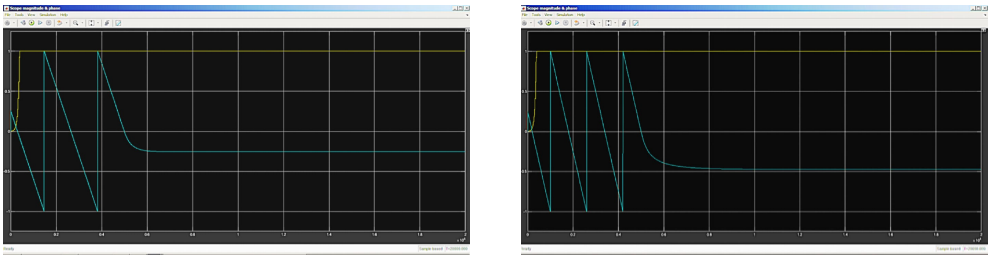

(a) (b)

Figure 30: Magnitude (yellow) and phase (blue) relative to the RF source of the OE Oscillator. The theoretical prediction of $\tan(\omega\tau) = -0.0985$

Figure 30a shows a plot of the magnitude and phase with respect to the RF source of the OE Oscillator under the same conditions of injection as in Figure 29. In the first 5000 μs the oscillator is freely oscillating at a lower frequency than the RF source so that its relative phase is a ramp with negative slope which modulo of 2π is wrapped into a sawtooth waveform. After 5000 μs the relative phase decays to a constant confirming successful phase locking. Figure 30b shows that the OE Oscillator is tuned to a nominal

reference frequency. The RF source is detuned to a higher frequency limit of the locking range $|\omega\tau| < \sin^{-1}\rho$ for an injection ratio ρ =0.1. The asymptotic phase $\theta_\infty = -0.4734\pi$ which gives $\tan(\omega\tau) = -0.098$.

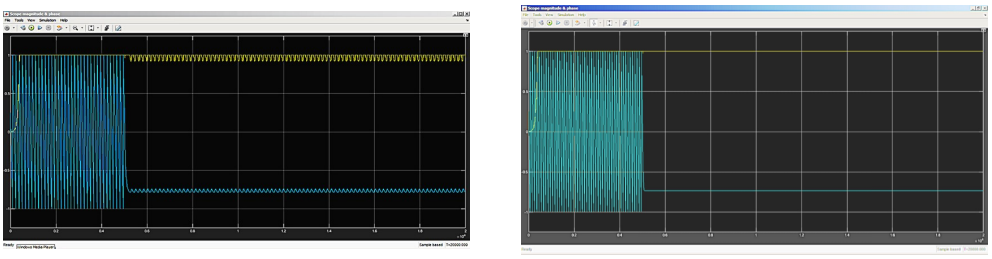

(a) ρ =0.9 (b) ρ=1.5

Figure 31: Magnitude (yellow) and phase (blue) relative to the RF source of the OE Oscillator with their respective injection ratio

Figure 31a shows the magnitude and phase relative to the RF source of the OE Oscillator for the same conditions as in Figure 30 except the injection ratio is increased to ρ=0.9 with a commensurate increase in the detuning of the RF source. Loss of amplifier saturation is observed which results in a ripple of the relative magnitude and phase albeit not without complete loss of lock. The ripple may be eliminated by increasing the linear gain of the sustaining amplifier sufficiently to restore saturation. An increase from 1.5 to 1.75 is sufficient in this example. The conjecture that loss of saturation during a destructive interference may be neglected provided the detuning is within the locking range appears correct only in the sense of convergence to the rippled phase state: a rigidly locked state requires maintenance of saturation.

Figure 31b shows the magnitude and phase relative to the RF source of

the OE Oscillator for an injection ratio ρ =1.5 with the detuning within an interval of half a free-spectral range about zero. This detuning interval ensures that the nominal reference frequency corresponds to the free oscillator mode closest in frequency to the RF source. It is observed that successful locking may also be achieved with an injection ratio exceeding unity with the same condition concerning amplifier saturation.

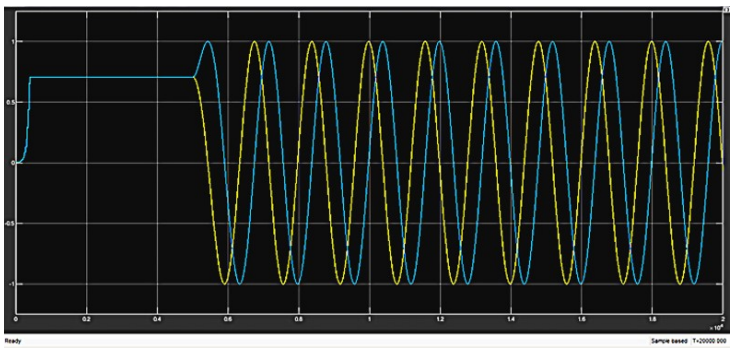

Figure 32: Lock-in range

Lastly, to determine the locking range it is convenient to tune the OE Oscillator to the nominal reference frequency. The envelope is then a complex constant in the absence of injection (indicated by the flat line) as shown in Figure 32. Locking occurs for detuning of the RF source satisfying $|\omega\tau| < \sin^{-1}\rho$.

4.2.5 Phase noise analysis

This section deals with the analysis of phase noise performance of the injection locked OE Oscillator. In theory, the injection locking process with the frequency multiplication scenario where a low frequency oscillator (say 100

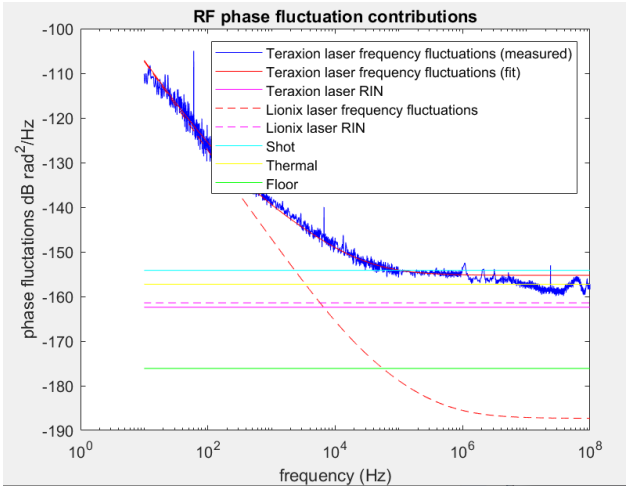

Figure 33: Open loop phase noise contributions induced by different noise sources corresponding to the components and model

MHz) is multiplied up in frequency, increases its phase noise spectral density by a factor of 20[Log(N)] dB. Whereas, using a multiplied quartz crystal oscillator will nevertheless have lower frequency phase noise than a free OE Oscillator but there is an offset frequency of a few 100 Hz where the free OE Oscillator will have lower phase noise than the multiplied source [71]. So if one uses a multiplied system reference to injection lock an OE Oscillator without a deterioration of the phase noise one must choose the injection ratio to be sufficiently smaller that the OE Oscillator such that it is essentially free beyond a few 100 Hz offset. The risk with such weak locking is that some perturbation (e.g. vibration) knocks the system out of lock [74].

A. Analysis of Noise Contributors -

To study and evaluate phase noise performance of a single loop OE Oscillator, simulations are performed using MATLAB. The open loop phase noise

contributions from the selected components are shown in Figure 33. Here two different lasers are used: Teraxion laser having frequency tuning range of ± 25 GHz and RIN of < -160 dBc/Hz [72]. And the second laser used is the Lionix laser having a RIN of -140 dBc/Hz and output power upto 85 mW [73]. The parameters used for the simulation are listed in Table 2.

Simulation parameters	Values
Photodiode impedance (Z)	50 Ohm
Photodiode current (A)	6 mA
RF signal power (P_{RF})	8 dBm
Length of the optical fibre (l)	5 km
Optical fiber group index (n_g)	1.45
Modulation index (m)	2.425
Peak RF voltage (V_{RF})	2.23 V
Phase bias (ϕ)	0.53
Optical fiber delay (t_d)	4.83 ns
Dispersion ratio (d)	17 μs/m
Responsivity (R)	0.56 A/W
Oscillation frequency (f)	10 GHz

Table 2: List of parameters used in OE Oscillator prototype simulation

B. Predicted phase noise performance of the prototype -

To confirm the phase noise model for a single loop SSB OE Oscillator, a comparison between the predicted phase noise and prototype phase noise is performed. This comparison is presented in the Figure 34, where the phase

noise prototype pretty much agrees with the predicted model. The low level of the spurs, -103 dBc/Hz at 40kHz offset frequency has to be noted. However some discrepancies can be noticed at frequencies > 1MHz, owing to either the low resolution of the measurement bench or Rayleigh scattering and hence, missed the prediction. A careful observation of the simulation indicates that the phase noise between 10 Hz to 5KHz has a consistent slope of 1/f for the Teraxion laser which is converted to $1/f^3$ by the integrating action. Having matched these results to the one from Figure 33, the open loop noise sources such as the phase noise induced by laser frequency noise and RF amplifier noise have contributed to the slope.

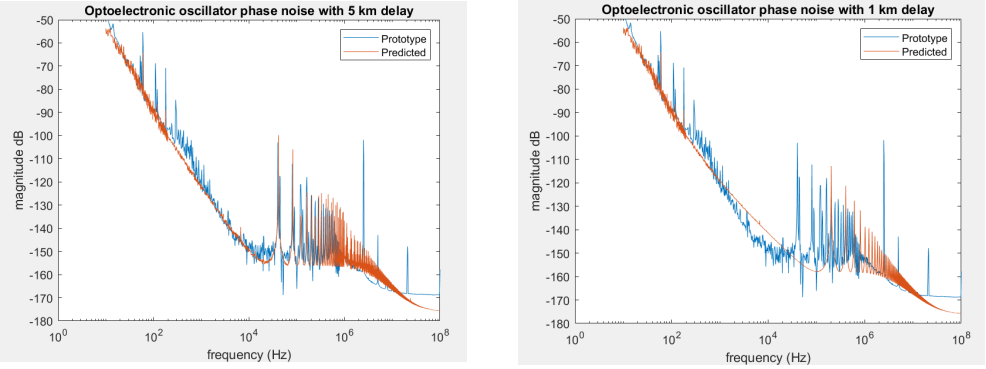

(a) (b)

Figure 34: Closed loop phase noise of the single loop OE Oscillator at 10 GHz (a) with 5 km delay line, the spurs present at frequencies > 1 MHz caused by the lazer frequency noise or RF amplifier noise. (b) with 1 km delay line, spurs caused because of the phase noise measurement bench

According to the model, the 5km long fiber has slightly better phase noise between the frequency set 10^2 to 10^4 when compared to 1 km long fiber

shown in the Figure 34b. But this is at the cost of the spurs being close to the carrier [79]. The factor that influences the noise for the lower frequency part of the spectrum is the increased laser frequency noise contribution [75]. This is independent of the fiber length; longer delay lines helps reduce the phase noise due to other mechanisms, but also contributing accordingly to the noise distribution. Thus, analysing the phase noise performance of an oscillator helps in optimising the performance of each of its component [76].

To evaluate the other major factor contributing to the phase noise analysis, consider the optical power output of the Mach-Zehnder Modulator (MZM) to be $P_{out(mod)}$ nominally biased at its maximum transmission point is described as:

$$P_{out(mod)} = P_{peak}\frac{1}{2}\left(1 + cos\left[\frac{\pi}{V_\pi}(V_{in} + V_B)\right]\right) \tag{59}$$

where P_{peak} is the peak optical power incident on the photodetector, V_{in} is the input RF oscillation that is define by $V_{in} = V_{RF}cos(\omega t)$, where ω is the angular RF frequency. Substituting the value of V_{in} in equation (59) an invoking Jacobi Anger expansion, the values of power can be obtained, where $P_{0(mod)}$ acts a constant and $P_{1(mod)}$ as a carrier component.

$$P_{0(mod)} = \frac{1}{2}P_{peak}\left[1 + cos\left(\frac{\pi V_B}{V_\pi}\right)J_0(m)\right] \tag{60}$$

$$P_{1(mod)}cos(\omega t) = P_{peak}\left[sin\left(\frac{\pi V_B}{V_\pi}\right)J_1(m)cos(\omega t)\right] \tag{61}$$

where $J_0(m)$ and $J_1(m)$ are the Jacob Anger constants and m= $\pi V_{RF}/V_\pi$ and the value of V_B being biased at one of the quadrature transmission points is given by $\pm V_\pi/2$. Substituting the values in Equation 60 and 61:

$$P_{0(mod)} = (1/2)P_{peak} \tag{62}$$

$$P_{1(mod)} = P_{peak} J_1(m) \tag{63}$$

The bias drift factor χ can be written as the ratio of $P_{0(mod)}$ and $P_{1(mod)}$, using equation (60) and equation (61)

$$\chi = \frac{sin(\pi V_B / V_\pi)}{1 + cos(\pi V_B / V_\pi)} * \frac{2J_1(m)}{J_0(m)m} \tag{64}$$

When the bias drift factor is large, it causes the oscillator power to vary and eventually leads to mode hopping. Hence, in a long term operation of an OE Oscillator, bias stabilisation and tracking becomes necessary [78].

4.3 Summary

Most of the previous research performed on OE Oscillator produced single loop OE Oscillator model using simulink. The models were analysed theoretically and experimentally with injection locking characteristics. Our research aimed at elucidating and characterising single loop OE Oscillator and its injection locking model using simulink and matlab for time- and frequency-domain models respectively. This chapter explicitly explains each block used in the simulink model and its work flow. Simulation results included in the OE Oscillator model is the in-phase (real) and quadrature phase (imaginary) components of the complex envelope. Followed by simulations on the injection locking model, presenting the magnitude and phase simulations relative to the RF source of the OE Oscillator under different injection ratio conditions. Based on detuning the RF source to 98% of the high frequency limit of the locking range given by $\omega\tau < sin^{-1}\rho$, the locking is accomplished. The real and imaginary parts of the OE Oscillator RF out complex envelope under injection locking condition was also presented. Finally, the phase

noise performance is predicted considering all noise mechanisms that enabled achievement of state-of-the-art phase noise performance (< -150 dB/Hz @ 10 kHz).

5 Summary and conclusion

5.1 Summary

Overall by the end of the research work, one can understand that the principle challenge is to understand and achieve world-class performance optoelectronic oscillator (OE Oscillator). The goal is a tunable compact OE Oscillator with exceptionally low noise and high long-term stability targeting silicon photonic integration in one package [80]. The strategy is to trade aggressively reduced noise for more compact components. The performance of novel oscillator architectures combined with noise suppression methods has been evaluated through theoretical modeling and verification by simulation. This architecture is enabled by an original solution to the tuning of interferometers and oscillators.

Laser noise drives many of the noise mechanisms within an OE Oscillator. Serendipitously, both laser and OE Oscillator are examples of the same class of oscillator so similar noise reduction techniques may be applied to lasers for OE Oscillator and other applications. There is a strong expectation of the generation of new knowledge in areas as diverse as: component noise mechanisms, noise measurement, noise suppression methods, automatic tuning control, coupled oscillator dynamics, and optoelectronic and electro-optic device hybridisation with silicon photonics [77]. The noise and long-term stability of the system oscillator is of major importance in applications such as optical and wireless communications, radar and lidar systems and astronomy. The results of this research will benefit Canada by supporting the growth in Information and Communication technology (ICT) critical to a knowledge-

based digital economy. It will contribute directly to wealth creation through new products and processes with an open market impact.

5.2 Conclusion

In conclusion, we have studied the complete model of an OE Oscillator and the injection locking phenomenon. We have studied the phase locking dynamics of the single loop OE Oscillator having the least amplitude perturbation effect. These OE Oscillators have a low phase noise performance measured at -103 dBc/Hz at 40 KHz offset frequency for a single loop OE Oscillator. We can conclude that as the frequency of the injection signal comes close enough to the frequency of the oscillator carrier that is maintained by injection signal amplitude, the beat frequency decreases gradually and becomes zero. At this point the oscillator loses its identity and becomes locked to the injection signal. The performance of an OE Oscillator is driven by the advantage of Phase locked Loop (PLL) technique. These PLL influenced OE Oscillator are amendable to monolithic integration using silicon photonics that guarantees compact, low noise, low cost, high performance solution. A superior performance can be expected by using a long delay line having low loss that suppresses the spurious oscillations.

Since, the optical delay lines are intrinsically temperature sensitive, it becomes necessary to have a control circuit to regulate the effective fiber length that prevent the mode hopping phenomenon. An active degenerative feedback that controls the carrier phase noise along with self injection and mode locking technique will prove to be a fixating breakthrough that not only produces uniform mode fixed performance but also reducing the frequency

drift due to operations changes. This injection locking analysis can also be used to generate OE Oscillator based clock recovery [7], low RF signal detection under low noise conditions, generation of high spectral purity RF oscillations in high frequency domain. In addition to this, this study will enable researcher to explore more in the field of phase-locking phenomenon using dual-loop OE Oscillator architecture and its phase noise performance evaluation. We can also extend this study to analyzing the phase locking dynamics of an OE Oscillator under the influence of stronger injection signals.

5.3 Suggestions for future work

5.3.1 Using optimal fiber length and improved optics Link

In the previous chapters, we discussed about injection locked OE Oscillator using long delay lines that results in side-mode suppression while maintaining the phase noise performance. The system contains residual noise that hinders the performance of the OE Oscillator. This residual noise gets multiplied with the transfer function and this product becomes dominant close-in to the carrier phase noise. We know that the magnitude of the transfer function is inversely proportional to the delay line length. Hence, the delay line is longer, the magnitude of the transfer function is lower and the contribution from residual noise is reduced. However, when the delay length increases, the reduction is the oscillator phase noise tends to get over-powered by the system residual noise in the close-in offset region. Adding to this condition, when the delay line is longer than desired, the phase noise starts to degrade due to high loss resulting in increased noise to signal ratio at the output. As

discussed in Chapter 3, a system that uses a laser having a RIN value of -135 dB/Hz results in RIN dominated system [33]. If a better laser with a higher RIN level of about -170 dB/Hz is used [65], it is likely like that the shot noise will tend to dominate. In such a case increasing the optical power will reduce the noise to signal ratio and improve the phase noise performance.

5.3.2 Temperature regulated environment for noise measurement

The long fiber loops used in the OE Oscillators are sensitive temperature, which when not taken into account can results in fluctuation of the operating frequency by tens of kilo hertz. A solution that records the oscillation frequency as well as the optical fiber temperature was introduced based on the vector network analyzer. The fluctuations are recorded as specific variations such as in the refractive index or length of the fiber. In case of the injection locking process, the temperature fluctuation causes the oscillator frequency to drift, resulting is poor thermal stability [67]. The variation in the oscillator frequency (f) with respect to the temperature changes ($\triangle T$) can be expressed as:

$$\frac{\triangle f}{f \triangle T} = -K_b \left[\left(\frac{\triangle n}{n \triangle T} \right) + \left(\frac{\triangle L}{L \triangle T} \right) \right] \tag{65}$$

where K_b is the Boltsman's constant and n is the refractive index and L is the length of the fiber delay line. The aim is to reduce the temperature sensitivity of the optical fiber based OE Oscillator using active temperature compensation techniques. A number of methods including the use of solid core photonic crystal fiber [68], composite fiber structure consisting of silica based fiber cascaded with a hollow core photonic crystal fiber [69], photonic

crystal fibers with air voids [70] has been proposed till date. Although these methods have proven to be useful in achieving thermal stability, it results in degradation in the close-in to carrier phase noise and excessive optical loss. A viable solution to such problems has been on debate for over a decade and still continue to create a platform for new researches.

5.3.3 Optical filtering

Another proposed method to effectively suppress the side-modes peaks in the use of optical transverse filters or Mach-Zehnder Interferometer (MZI) [40]. An optical resonator/ filter technique ensures small size, low cost, low loss for higher order, inherent narrow bandwidth and easy tunability.

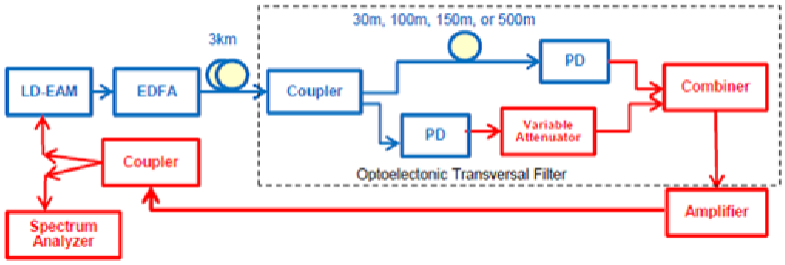

Figure 35: The use of Optical transverse filter in an Oscillator setup

As shown in Figure 35 this optical resonator filters the RF signal in optical domain in the microwave parts of the loop. This way it behaves as a classical oscillator with an optical filter instead of a delay line. The operating frequency in this system will be equal to the free spectral range (FSR) of the resonator [40]. However, with such a setup it is difficult to calculate the change in the refractive index and hence, a solution to this problem leads to

the direction of research and development.

6 References

[1] X. S. Yao and L. Maleki. "Optoelectronic microwave oscillator." Journal of the Optical Society of America B 13.8 (1996): 1725-1735.

[2] T. J. Hall, C. W. T Nicholls, B. Spokoinyi, M. Hasan, "High stability optoelectronic oscillator and method." US Patent Apl. No. 62/886,039, 13 Aug. 2009.

[3] T. Hao, J. Tang, D. Domenech, W. Li, N. Zhu, J. Capmany and M. Li. "Toward monolithic integration of OE Oscillators: From systems to chips." Journal of Lightwave Technology 36.19 (2018): 4565-4582.

[4] O. Lelièvre, V. Crozatier, P.Berger, G. Baili, O. Llopis, D. Dolfi, G. Pillet, P. Nouchi, F. Goldfarb, F. Bretenaker, L. Morvan. "A model for designing ultralow noise single-and dual-loop 10-GHz optoelectronic oscillators." Journal of Lightwave Technology 35.20 (2017): 4366-4374.

[5] K. Mikitchuk, A. Chizh and S. Malyshev. "Delay-line optoelectronic oscillator with all-optical gain." 2016 46th European Microwave Conference IEEE (2016).

[6] A. Liu, J. Dai, and K. Xu. "Stable and low-spurs optoelectronic oscillators: A review." Applied Sciences 8.12 (2018): 2623.

[7] A. Banerjee, and B. Biswas. "Analysis of phase-locking in optoelectronic

microwave oscillators due to small RF signal injection." IEEE Journal of Quantum Electronics 53.3 (2017): 1-9.

[8] D. B. Leeson. "Oscillator phase noise: a 50-year review." IEEE transactions on Ultrasonics, Ferroelectrics, and Frequency Control 63.8 (2016): 1208-1225.

[9] D. Eliyahu, D. Seidel, and L. Maleki. "Phase noise of a high performance OE Oscillator and an ultra low noise floor cross-correlation microwave photonic homodyne system." 2008 IEEE International Frequency Control Symposium (2008).

[10] Chembo, Y. Kouomou, L. Larger, and P. Colet. "Nonlinear dynamics and spectral stability of optoelectronic microwave oscillators." IEEE Journal of Quantum Electronics 44.9 (2008): 858-866.

[11] S. X. Yao, and L. Maleki. "Opto-electronic oscillator and its applications." International Topical Meeting on Microwave Photonics. MWP'96 Technical Digest. Satellite Workshop (Cat. No. 96TH8153) IEEE (1996).

[12] E. C. Levy, M. Horowitz, and C. R. Menyuk. "Modeling optoelectronic oscillators." Journal of the Optical Society of America B 26.1 (2009): 148-159.

[13] Y. Liu, T. Hao, W. Li, J. Capmany, N. Zhu, and M. Li. "Observation of parity-time symmetry in microwave photonics." Light: Science and

Applications 7.1 (2018): 1-9.

[14] L. Huang, L. Deng, S. Fu, M. Tang, M. Cheng, M. Zhang, and D. Liu. "Stable and compact dual-loop optoelectronic oscillator using self-polarization-stabilization technique and multicore fiber." Journal of Lightwave Technology 36.22 (2018): 5196-5202.

[15] S. X. Yao, and L. Maleki. "Dual microwave and optical oscillator." Optics Letters 22.24 (1997): 1867-1869.

[16] W. Zhou, and G. Blasche. "Injection-locked dual opto-electronic oscillator with ultra-low phase noise and ultra-low spurious level." IEEE Transactions on Microwave Theory and Techniques 53.3 (2005): 929-933.

[17] L. Huo, Y. Dong, C. Lou, and Y. Gao. "Clock extraction using an optoelectronic oscillator from high-speed NRZ signal and NRZ-to-RZ format transformation." IEEE Photonics Technology Letters 15.7 (2003): 981-983.

[18] N. Yu, E. Salik, and L. Maleki. "Ultralow-noise mode-locked laser with coupled optoelectronic oscillator configuration." Optics Letters 30.10 (2005): 1231-1233.

[19] S. X. Yao, and L. Maleki. "Multiloop optoelectronic oscillator." IEEE Journal of Quantum Electronics 36.1 (2000): 79-84.

[20] Y. Jiang, G. Bai, L. Hu, H. Li, Z. Zhou, J. Xu, and S. Wang. "Frequency locked single-mode optoelectronic oscillator by using low frequency RF signal injection." IEEE Photonics Technology Letters 25.4 (2013): 382-384.

[21] K. Saleh, P. H. Merrer, O. Llopis, and G. Cibiel. "Optical scattering noise in high Q fiber ring resonators and its effect on optoelectronic oscillator phase noise." Optics Letters 37.4 (2012): 518-520.

[22] A. F. Talla, R. Martinenghi, G. R. Goune Chengui, J. H. Talla Mbé, K. Saleh, A. Coillet, G. Lin, P. Woafo, and Y. K. Chembo. "Analysis of phase-locking in narrow-band optoelectronic oscillators with intermediate frequency." IEEE Journal of Quantum Electronics 51.6 (2015): 1-8.

[23] S. Huang, L. Maleki, and T. Le. "A 10 GHz optoelectronic oscillator with continuous frequency tunability and low phase noise." IEEE International Frequncy Control Symposium and PDA Exhibition (Cat. No. 01CH37218) (2001): 720-727.

[24] D. B. Sullivan, D. W. Allan, D. A. Howe, and F. L. Walls. "Characterization of clocks and oscillators." Technical Note: National Institute of Standards and Technology (1990).

[25] W. F. Walls. "Cross-correlation phase noise measurements." In Proceedings of the 1992 IEEE Frequency Control Symposium (1992): 257-261.

[26] A. Chenakin "Phase noise reduction in microwave oscillators." Microwave J 52.10 (2009): 124-140.

[27] D. Allan, H. Hellwig, P. Kartaschoff, J. Vanier, J. Vig, G. M-R Winkler, and N. F. Yannoni. "Standard terminology for fundamental frequency and time metrology." Proceedings of the 42nd Annual Frequency Control Symposium IEEE (1988): 419-425.

[28] E. S. Ferre-Pikal, J. R. Vig, J. C. Camparo, L. S. Cutler, L. Maleki, W. J. Riley, S. R. Stein, C. Thomas, F. L. Walls, and J. D. White. "Draft revision of IEEE STD 1139-1988 standard definitions of physical quantities for fundamental, frequency and time metrology-random instabilities." Proceedings of International Frequency Control Symposium IEEE (1997): 338-357.

[29] E. Rubiola, "Phase noise and frequency stability in oscillators." Cambridge University Press (2009).

[30] S. Romisch, J. Kitching, E. Ferre-Pikal, L. Hollberg, and F. L. Walls. "Performance evaluation of an optoelectronic oscillator." IEEE Transactions on Ultrasonics, Ferroelectrics, and Frequency control 47.5 (2000): 1159-1165.

[31] K. Volyanskiy, Y. K. Chembo, L. Larger, and E. Rubiola. "Contribution of laser frequency and power fluctuations to the microwave phase noise of optoelectronic oscillators." Journal of Lightwave Technology 28.18 (2010):

2730-2735.

[32] R. Paschotta. "Encyclopedia of laser physics and technology." Vol. 1 Berlin: Wiley-vch (2008).

[33] A. Gubenko, A. Kovsh, G. Wojcik, D. Livshits, I. Krestnikov, and S. Mikhrin. "Semiconductor laser with low relative intensity noise of individual longitudinal modes and optical transmission system incorporating the laser." U.S. Patent No. 8,411,711. 2 Apr. 2013.

[34] O. Lelièvre, V. Crozatier, G. Baili, P. Berger, G. Pillet, D. Dolfi, L. Morvan, F. Goldfarb, F. Bretenaker, and O. Llopis. "Ultra low noise 10 GHz dual loop optoelectronic oscillator: experimental results and simple model." 2016 IEEE International Frequency Control Symposium (2016): 1-5.

[35] L. Jacubowiez, J. Roch, J. Poizat, and P. Grangier. "Teaching photodetection noise sources in laboratory." Proceedings-Spie The International Society for Optical Engineering (1997): 166-179.

[36] W. K. Marshall, B. Crosignani, and A. Yariv. "Laser phase noise to intensity noise conversion by lowest-order group-velocity dispersion in optical fiber: exact theory." Optics Letters 25.3 (2000): 165-167.

[37] R. M. Shelby, M. D. Levenson, and P. W. Bayer. "Guided acoustic-wave Brillouin scattering." Physical Review B 31.8 (1985): 5244.

[38] N. K. Raut, J. Miller, and J. Sharping. "Progress in Optoelectronic Oscillators." Journal of Institute of Science and Technology 24.1 (2019): 26-33.

[39] E. Rubiola, E. Salik, N. Yu, and L. Maleki. "Flicker noise in high-speed pin photodiodes." IEEE Transactions on Microwave Theory and Techniques 54.2 (2006): 816-820.

[40] P. Devgan. "A review of optoelectronic oscillators for high speed signal processing applications." ISRN Electronics (2013).

[41] J. R. Vig, E. S. Ferre-Pikal, J. C. Camparo, L. S. Cutler, L. Maleki, W. J. Riley, S. R. Stein, C. Thomas, F. L. Walls, and J. D. White. "IEEE standard definitions of physical quantities for fundamental frequency and time metrology-random instabilities." IEEE Standard 1139 (1999): 1999.

[42] J. Yang, Y. Jin-Long, W. Yao-Tian, Z. Li-Tai, and Y. En-Ze. "An optical domain combined dual-loop optoelectronic oscillator." IEEE Photonics Technology Letters 19.11 (2007): 807-809.

[43] J. H. Cho, H. Kim, and H. Sung. "Reduction of spurious tones and phase noise in dual-loop OE Oscillator by loop-gain control." IEEE Photonics Technology Letters 27.13 (2015): 1391-1393.

[44] M. Fleyer, A. Sherman, M. Horowitz, and M. Namer. "Wideband-frequency tunable optoelectronic oscillator based on injection locking to an electronic oscillator." Optics Letters 41.9 (2016): 1993-1996.

[45] O. Okusaga, E. J. Adles, E. C. Levy, W. Zhou, G. M. Carter, C. R. Menyuk, and M. Horowitz. "Spurious mode reduction in dual injection-locked optoelectronic oscillators." Optics Express 19.7 (2011): 5839-5854.

[46] E. C. Levy, O. Okusaga, M. Horowitz, C. R. Menyuk, W. Zhou, and G. M. Carter. "Comprehensive computational model of single-and dual-loop optoelectronic oscillators with experimental verification." Optics Express 18.20 (2010): 21461-21476.

[47] D. Eliyahu, and L. Maleki. "Low phase noise and spurious level in multi-loop opto-electronic oscillators." In IEEE International Frequency Control Symposium and PDA Exhibition Jointly with the 17th European Frequency and Time Forum (2003): 405-410.

[48] H. Peng, H. Du, R. Guo, Y. Xu, C. Zhang, J. Chen, and Z. Chen. "Highly Stable and Low Phase Noise 10 GHz RF Signal Generation Based on a Sub-Harmonic Injection Locked Optoelectronic Oscillator." IEEE International Frequency Control Symposium (2018): 1-3.

[49] D. B. Leeson. "Oscillator phase noise: A 50-year retrospective." Joint Conference of the IEEE International Frequency Control Symposium the

European Frequency and Time Forum (2015): 332-337.

[50] H. J. Peppiatt, J. A. Hall, and A. V. McDaniel. "A low-noise class-C oscillator using a directional coupler." IEEE Transactions on Microwave Theory and Techniques 16.9 (1968): 748-752.

[51] J. A. Mullen. "Background noise in nonlinear oscillators." Proceedings of the IRE 48.8 (1960): 1467-1473.

[52] R. Adler. "A study of locking phenomena in oscillators." Proceedings of the IEEE 61.10 (1973): 1380-1385.

[53] L. J. Paciorek. "Injection locking of oscillators." Proceedings of the IEEE 53.11 (1965): 1723-1727.

[54] R. C. Mackey. "Injection locking of klystron oscillators." IRE Transactions on Microwave Theory and Techniques 10.4 (1962): 228-235.

[55] A. Hajimiri. "Noise in phase-locked loops." Southwest Symposium on Mixed-Signal Design (Cat. No. 01EX475) IEEE (2001): 1-6.

[56] Z. Zhou, Y. Chun, C. Zhewei, C. Yuhua, and L. Xianghua. "An ultra-low phase noise and highly stable optoelectronic oscillator utilizing IL-PLL." IEEE Photonics Technology Letters 28.4 (2015): 516-519.

[57] K. H. Lee, J. Y. Kim, and W. Y. Choi. "Injection-locked hybrid optoelectronic oscillators for single-mode oscillation." IEEE Photonics Technology Letters 20.19 (2008): 1645-1647.

[58] J. Sarkar, A. Banerjee, and B. Biswas. "Analysis of frequency pulling phenomenon in an optoelectronic oscillator." Optical Engineering 57.6 (2018): 067102.

[59] B. Hong, and A. Hajimiri. "A general theory of injection locking and pulling in electrical oscillators—Part I: Time-synchronous modeling and injection waveform design." IEEE Journal of Solid-State Circuits 54.8 (2019): 2109-2121.

[60] F. Jiang, J. H. Wong, H. Q. Lam, J. Zhou, S. Aditya, P. H. Lim, K. E. K. Lee, P. P. Shum, and X. Zhang. "An optically tunable wideband optoelectronic oscillator based on a bandpass microwave photonic filter." Optics Express 21.14 (2013): 16381-16389.

[61] K. H. Lee, J. Y. Kim, and W. Y. Choi. "A 30-GHz self-injection-locked oscillator having a long optical delay line for phase-noise reduction." IEEE Photonics Technology Letters 19.24 (2007): 1982-1984.

[62] L. C. Archundia, and P. J. Delfyett. "External cavity multiwavelength semiconductor mode-locked lasers gain dynamics." Optics Express 14.20 (2006): 9223-9237.

[63] M. Shi, L. Yi, W. Wei and W. Hu. "Generation and phase noise analysis of a wide optoelectronic oscillator with ultra-high resolution based on stimulated Brillouin scattering." Optics Express 26.13 (2018): 16113-16124.

[64] G. J. Schneider, J. A. Murakowski, C. A. Schuetz, S. Shi, and D. W. Prather. "Radiofrequency signal-generation system with over seven octaves of continuous tuning." Nature Photonics 7.2 (2013): 118.

[65] Li. Zhang, A. Poddar, U. Rohde, and A. S. Daryoush. "Phase noise reduction and spurious suppression in oscillators utilizing self-injection loops." IEEE Radio and Wireless Symposium (2014): 187-189.

[66] J. W. Fisher, L. Zhang, A. Poddar, U. Rohde, and A. S. Daryoush. "Phase noise performance of optoelectronic oscillator using optical transversal filters." IEEE Benjamin Franklin Symposium on Microwave and Antenna Sub-systems for Radar, Telecommunications, and Biomedical Applications (2014): 1-3.

[67] T. Musha, J. Kamimura, and M. Nakazawa. "Optical phase fluctuations thermally induced in a single-mode optical fiber." Applied Optics 21, no. 4 (1982): 694-698.

[68] M. Kaba, H-W. Li, A. S. Daryoush, J-P. Vilcot, D. Decoster, J. Chazelas, G. Bouwmans, Y. Quiquempois, and F. Deborgies. "Improving thermal sta-

bility of opto-electronic oscillators." IEEE Microwave Magazine 7.4 (2006): 38-47.

[69] A. S. Daryoush, H. W. Li, M. Kaba, G. Bouwmans, D. Decoster, J. Chazelas, and F. Deborgies. "Passively temperature stable opto-electronic oscillators employing photonic crystal fibers." In Proceedings of the European Microwave Association 3.3 (2007): 201-209.

[70] G. Beck, L. Bigot, G. Bouwmans, A. Kudlinski, J-P. Vilcot, and M. Douay. "Benefits of photonic bandgap fibers for the thermal stabilization of optoelectronic oscillators." IEEE Photonics Journal 4.3 (2012): 789-794.

[71] H. Peng, C. Zhang, X. Xie, T. Sun, P. Guo, X. Zhu, L. Zhu, W. Hu, and Z. Chen. "Tunable DC-60 GHz RF generation utilizing a dual-loop optoelectronic oscillator based on stimulated Brillouin scattering." Journal of Lightwave Technology 33.13 (2015): 2707-2715.

[72] C. Sun, S. Xie, F. Liu, Y. Xie, W. Mao, B. Zhao, and H. Ge. "Integrated, module of a DFB laser and LiNbO3 modulator." Integrated Optoelectronics. International Society for Optics and Photonics 2891 (1996).

[73] H. Al-Taiy, N. Wenzel, S. Preußler, J. Klinger, and T. Schneider. "Ultra-narrow linewidth, stable and tunable laser source for optical communication systems and spectroscopy." Optics Letters 39.20 (2014): 5826-5829.

[74] P. Ghelfi, F. Laghezza, F. Scotti, G. Serafino, A. Capria, S. Pinna, D. Onori, C. Porzi, M. Scaffardi, A. Malacarne, V. Vercesi, E. Lazzeri, F. Berizzi, and A. Bogoni "A fully photonics-based coherent radar system." Nature 507.7492 (2014): 341-345.

[75] D. Zhu, T. H. Du, and S. L. Pan. "A coupled optoelectronic oscillator based on a resonant saturable absorber mirror." 32nd URSI General Assembly Science Symp (2017).

[76] A. Banerjee, L. A. D. de Britto, and G. M. Pacheco. "Analysis of Injection Locking and Pulling in Single-Loop Optoelectronic Oscillator." IEEE Transactions on Microwave Theory and Techniques 67.5 (2019): 2087-2094.

[77] A. Liu, J. Liu, J. Dai, Y. Dai, F. Yin, J. Li, Y. Zhou, T. Zhang, and K. Xu. "Spurious Suppression in Millimeter-Wave OE Oscillator With a High-Q Optoelectronic Filter." IEEE Photonics Technology Letters 29.19 (2017): 1671-1674.

[78] S. E. Hosseini, A. Banai, and F. X. Kärtner. "Low-drift optoelectronic oscillator based on a phase modulator in a Sagnac loop." IEEE Transactions on Microwave Theory and Techniques 65.7 (2017): 2617-2624.

[79] O. Lelièvre, V. Crozatier, P.Berger, G. Baili, O. Llopis, D. Dolfi, G. Pillet, P. Nouchi, F. Goldfarb, F. Bretenaker, L. Morvan. "A model for designing ultralow noise single-and dual-loop 10-GHz optoelectronic oscilla-

tors." Journal of Lightwave Technology 35.20 (2017): 4366-4374.

[80] Z. Li, A. Daryoush, A. Poddar, and U. Rohde. "Oscillator phase noise reduction using self-injection locked and phase locked loop (SILPLL)." IEEE International Frequency Control Symposium (2014): 1-4.